Journal of Volcanology and Geothermal Research, 22 (1984) 59—95
Elsevier Science Publishers B.V., Amsterdam — Printed in The Netherlands

SEISMICITY AT OLD FAITHFUL GEYSER: AN ISOLATED SOURCE OF GEOTHERMAL NOISE AND POSSIBLE ANALOGUE OF VOLCANIC SEISMICITY

SUSAN WERNER KIEFFER

U.S. Geological Survey, 2255 North Gemini Drive, Flagstaff, AZ 86001 (U.S.A.)

(Received February 1983; revised and accepted January 19, 1984)

ABSTRACT

Kieffer, S.W., 1984. Seismicity at Old Faithful Geyser: an isolated source of geothermal noise and possible analogue of volcanic seismicity. In: N. Oskarsson and G. Larsen (Editors), Volcano Monitoring. *J. Volcanol. Geotherm. Res.*, 22: 59—95.

Old Faithful Geyser in Yellowstone National Park, U.S.A., is a relatively isolated source of seismic noise and exhibits seismic behavior similar to that observed at many volcanoes, including "bubblequakes" that resemble B-type "earthquakes", harmonic tremor before and during eruptions, and periods of seismic quiet prior to eruptions. Although Old Faithful differs from volcanoes in that the conduit is continuously open, that rock-fracturing is not a process responsible for seismicity, and that the erupting fluid is inviscid H_2O rather than viscous magma, there are also remarkable similarities in the problems of heat and mass recharge to the system, in the eruption dynamics, and in the seismicity. Water rises irregularly into the immediate reservoir of Old Faithful as recharge occurs, a fact that suggests that there are two enlarged storage regions: one between 18 and 22 m (the base of the immediate reservoir) and one between about 10 and 12 m depth. Transport of heat from hot water or steam entering at the base of the recharging water column into cooler overlying water occurs by migration of steam bubbles upward and their collapse in the cooler water, and by episodes of convective overturn. An eruption occurs when the temperature of the near-surface water exceeds the boiling point if the entire water column is sufficiently close to the boiling curve that the propagation of pressure-release waves (rarefactions) down the column can bring the liquid water onto the boiling curve. The process of conversion of the liquid water in the conduit at the onset of an eruption into a two-phase liquid—vapor mixture takes on the order of 30 s. The seismicity is directly related to the sequence of filling and heating during the recharge cycle, and to the fluid mechanics of the eruption. Short (0.2—0.3 s), monochromatic, high-frequency events (20—60 Hz) resembling unsustained harmonic tremor and, in some instances, B-type volcanic earthquakes, occur when exploding or imploding bubbles of steam cause transient vibrations of the fluid column. The frequency of the events is determined by the length of the water column and the speed of sound of the fluid in the conduit when these events occur; damping is controlled by the characteristic and hydraulic impedances, which depend on the above parameters, as well as on the recharge rate of the fluid. Two periods of reduced seismicity (of a few tens of seconds to nearly a minute in duration) occur during the recharge cycle, apparently when the water rises rapidly through the narrow regions of the conduit, causing a sudden pressure increase that temporarily suppresses steam bubble formation. A period of decreased seismicity also precedes preplay or an eruption; this appears to be the time when rising steam bubbles move

into a zone of boiling that is acoustically decoupled from the wall of the conduit because of the acoustic impedance mismatch between boiling water ($\rho_c \sim 10^3$ g cm^{-2} s^{-1}) and rock ($\rho_c \sim 3 \times 10^5$ g cm^{-2} s^{-1}). Sustained harmonic tremor occurs during the first one to one-and-a-half minutes of an eruption of Old Faithful, but is not detectable in the succeeding minutes of the eruption. The eruption tremor is caused by hydraulic transients propagating within a sublayer of unvesiculated water that underlies the erupting two-phase liquid–vapor mixture. The resonant frequencies of the fluid column decrease to about 1 Hz when all of the water in the conduit has been converted to a water–steam mixture. Surges are observed in the flow at this frequency, but the resonance has not been detected seismically, possibly because the two-phase erupting fluid is seismically decoupled from the rock on which seismometers are placed. If Old Faithful is an analogue for volcanic seismicity, this study shows that because the frequency of tremor depends on the acoustic properties of the fluid and on conduit dimensions, both properties must be considered in analysis of tremor in volcanic regions. Because magma sound speed can vary over nearly two orders of magnitude as it changes from an undersaturated liquid into a saturated two-phase mixture, tremor frequency might vary by this magnitude and very broad-band seismographs may be required if tremor is to be monitored as magma goes from an undersaturated liquid to a vesiculated froth. Cessation of fluid-induced seismicity may indicate that the processes that drive the transients cease, but it is also possible that the processes that drive the transients continue but the fluid properties change so that the fluid becomes acoustically decoupled from the rock on which seismometers are placed.

INTRODUCTION

Volcanic seismicity that can specifically be attributed to activity of magma within conduits (in contrast to tectonic events or rock falls, for example) may have analogies in geyser systems that are amenable to detailed studies not possible at most volcanoes. A striking example of seismic similarity between volcanoes and geysers is shown in Fig. 1. The volcanic record from Karkar (Papua New Guinea) (Fig. 1a) shows "banded" seismic activity (McKee et al., 1981), that is very similar to the cyclic seismicity of Old Faithful in Yellowstone National Park, Wyoming, U.S.A. (Fig. 1b). Although this record of Old Faithful's activity was not available to McKee et al. (1981), they noted the similarity of the Karkar activity to geyser seismicity as described by Nicholls and Rinehart (1967) and postulated that a subterranean geyser system underlay Karkar. Not all volcanic seismicity is so remarkably similar to geyser seismicity as that of Karkar, but phenomena resembling volcanic B-type earthquakes and harmonic tremor do occur at some geysers. In this paper, I describe preliminary seismic studies on Old Faithful geyser and describe the relation of seismic activity to processes occurring before and during eruption. Old Faithful is probably one of the largest simple geysers that could be considered as a volcanic analogue; it is also a place where geothermal noise can be studied in relation to a single source of activity.

Seismicity at Old Faithful is related, in detail, to the sequence of events as the geyser empties, recharges with heat and water, and empties again through its eruption cycle. This report focuses on the seismic behavior, but draws on other data, particularly movie films collected by the author since

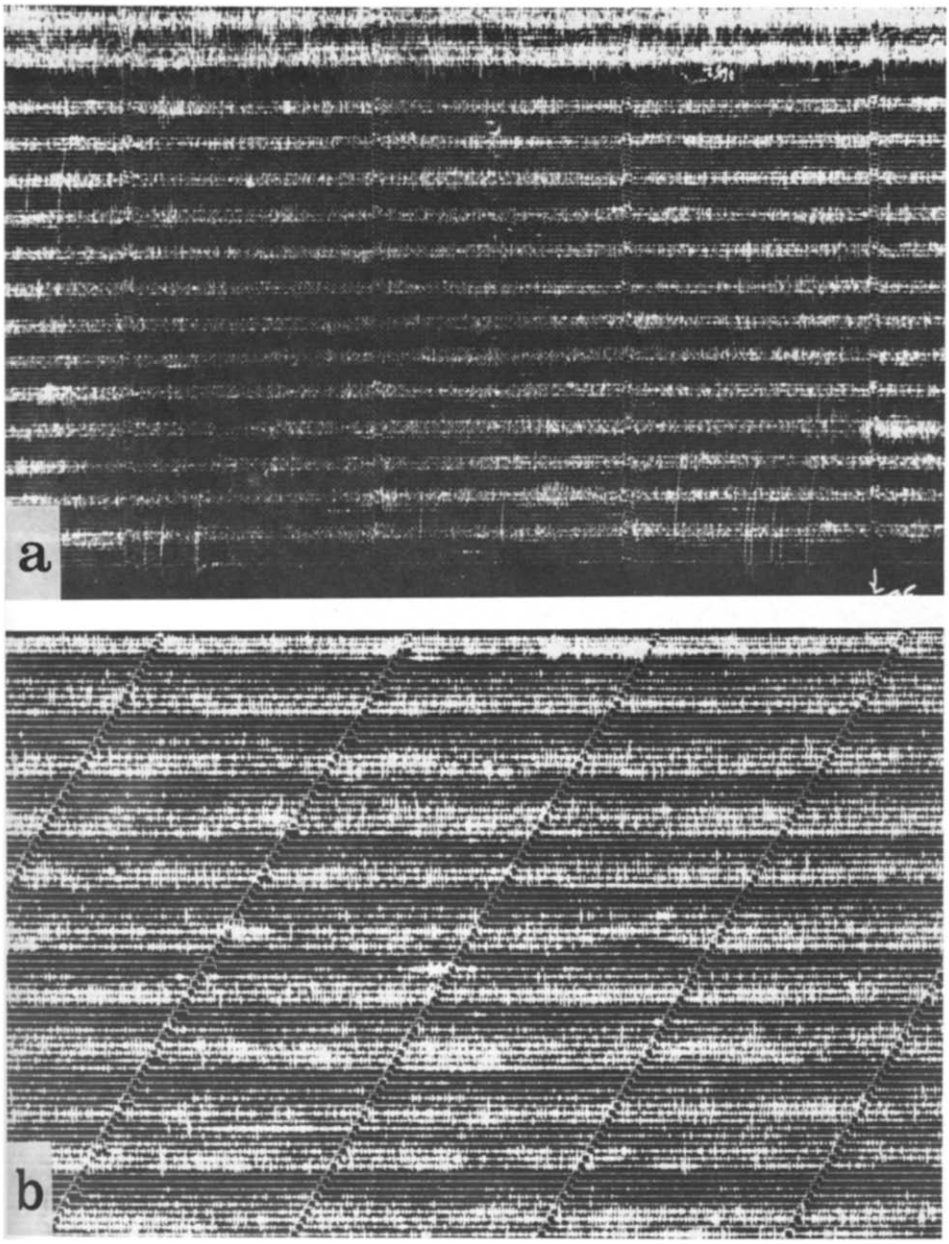

Fig. 1. a. "Banded" seismic activity at Karkar volcano, Papua New Guinea (from McKee et al., 1981, p. 65). The bands are stronger activity that recurs at intervals of about 70 min and at a frequency of 2—4 Hz. Seismogram provided by C. McKee and R.W. Johnson. b. Seismic activity at Old Faithful geyser, Yellowstone National Park. Ten and one-half eruption cycles are recorded. Time markers in (a) and (b) are at 1-min intervals.

1976, and thermocouple and float data obtained by Birch and Kennedy in 1948 (published in the 1972 reference listed, henceforth referred to as BK). The BK data are the only data currently available on temperature-depth relationships.

OBSERVATIONS AT OLD FAITHFUL

An eruption cycle

Old Faithful is a typical columnar geyser (Fig. 2). It erupts into a tall, continuous vertical jet of water and steam for periods of 1.5—5.5 min. The conduit is a fissure that is 1.52 × 0.58 m in horizontal dimensions ~0.5 m below the ground surface. Although the total length of the conduit is controversial, with proposed values ranging from 22 m (D.E. White, pers. commun., 1977; Birch and Kennedy, 1972) to 175 m (Rinehart, 1969), there is general agree-

Fig. 2. Old Faithful Geyser in Yellowstone National Park, U.S.A., during the stage of steady flow as defined in the text. Eruption column is about 30 m in height. Surges in the column are discussed in the text. Photo by Gonzalo Mendoza.

ment that the depth of the *immediate reservoir* open to the surface is about 22 m. Water fills the conduit only to within 6 m of the surface, so the maximum length of the water column in the reservoir immediately prior to eruption is about 16 m. Most erupted water runs off of the surface mound of sinter, so that direct recharge of water into the conduit from fallback is negligible.

An "eruption cycle" of Old Faithful consists of one eruption and one recharge interval; by convention, the start of a cycle is taken as the onset of an eruption. Visible surface play consists of four parts (Fig. 3):

(1) *preplay*: an interval prior to the actual eruption during which water is ejected for a few seconds in bursts to a few meters or even a few tens of meters height. Preplay typically begins 5—15 min before an eruption, but has been observed up to 30 min before an eruption (R. Hutchinson, pers. commun., 1983). It indicates vigorous upsurging of the top water in the conduit, and its effects are to bleed off and/or cool down some of the hot water from the top of the system, to lengthen the interval, and to postpone the eruption.

(2) *initiation and unsteady flow*: an interval of 20—40 s in which the eruption column develops and rises in a series of bursts (1 to 8 in number) to a height of 30—50 m.

(3) *steady flow*: an interval of about 30 s during which the column stays at maximum height. During this time, surging occurs at a frequency of 1—2 Hz (see Figs. 2 and 3).

(4) *decline*: an interval of up to 3 min in which the height of the column steadily drops to about 10 m and play continues at low levels. Long and short eruptions appear to be similar in stages 1, 2, and 3 above, and to differ only in the duration of this decline stage.

Eruption durations are not uniformly distributed over the range from 1.5 to 5.5 min, but rather, the distribution is bimodal (Fig. 4a). Short eruptions (less than 3 min) comprised about one-quarter of the total in 1979, the year of the seismic work reported (R. Hutchinson, pers. commun., 1983).

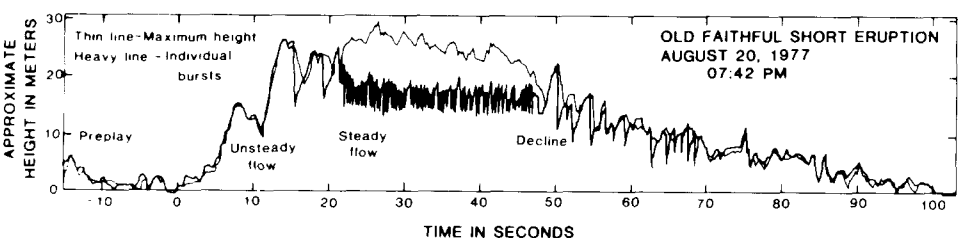

Fig. 3. A record of height versus time for a short eruption of Old Faithful, showing the four stages of eruption discussed in the text. Light line is height of the water—steam column; heavier line traces individual pulses of water, visible in Fig. 2, in order to obtain the frequency of this surging. By the convention used by Park Service personnel who record the onset and cessation of eruptions, time $t = 0$ is taken as the time after which water remains above the surface of the ground. The end of an eruption is the time at which the last liquid water is ejected.

A long eruption discharges more water from the geyser plumbing system and extracts more heat from the surrounding wall rocks than a short eruption. Therefore, the length of an interval, I, between eruptions, depends on the duration of the *previous* eruption, i.e., on the extent of the depletion of water and heat in the system. From statistical analysis on thousands of eruptions and intervals, Eugene Robertson (pers. commun., 1976) and R. Hutchinson (pers. commun., 1983) have documented the relation between the duration of an eruption, D, and the length of the following interval to be approximately:

$$I \sim 10\,D + 30 \qquad (1)$$

where all variables are expressed in minutes. Since this relation implies that the distribution of intervals will be the same as the distribution of durations, the distribution of intervals is a bimodal curve (Fig. 4b). The break in the curve that distinguished short from long intervals in 1979 was 64 min.

The distribution of durations and intervals of Old Faithful was different in 1979 (when the seismic data were obtained) than in 1948 (the year in which BK took their float and thermocouple data). In 1948, 50 min was the dividing time between intervals considered "short" and "long" (Rinehart, 1980), and only about ten percent of the eruptions were "short". The BK data were for an eruption following a 64-min interval. From U.S. Park Service records, I have estimated that this interval followed an eruption of 4 min. duration. This "long" interval of 1948 corresponds to one of the rare "medium"-length intervals of 1979 (see Fig. 4b). Therefore, in order to consider the possible correlations between the 1948 behavior and the 1979 behavior, seismic behavior through three representative eruption cycles are discussed:

(1) a *short* one of 56 min duration;
(2) a *medium* one of 66 min duration; and
(3) a *long* one of 76 min duration.

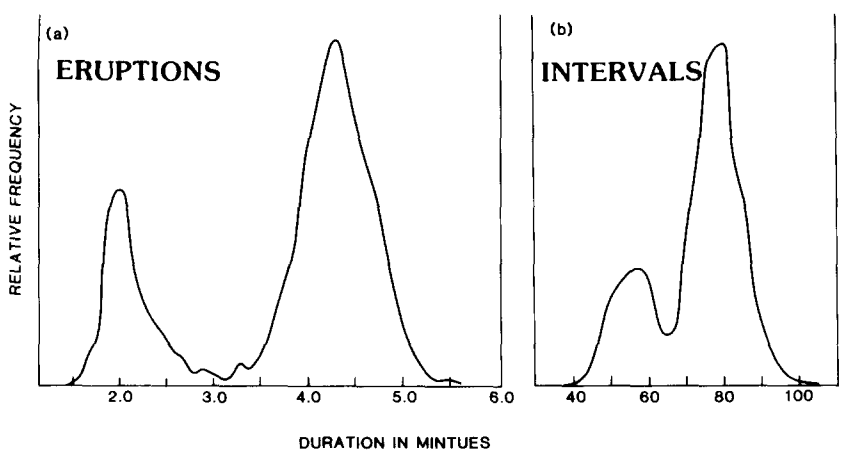

Fig. 4. a. The relative frequency of Old Faithful eruptions of various durations during the year 1979 (vertical scale, arbitrary units). b. The relative frequency of intervals between Old Faithful's eruptions (vertical scale, arbitrary units). Data provided by R. Hutchinson, U.S.N.P.S., from analysis of 3308 eruptions, 1983.

During the eruptions that preceeded the monitored intervals, Old Faithful apparently emptied below the 23-m level (see Fig. 5a for water levels). During the first 15 min of the recharge interval, the water level generally remained below 18 m, although it intermittently surged up to 15 m. After 32 min, it rose to the 15-m level, and at 34 min, to the 12-m level. The water stayed at a depth of 11—12 m from 34 to 54 min into the interval. Substantial surges in water level were observed, presumably as steam bubbles formed and dissipated in the conduit. From 58 min on to the eruption at 64 min, the water was at about 6 m depth; the eruption began with the water at this level, not at the ground surface. No reports of preplay were given by BK.

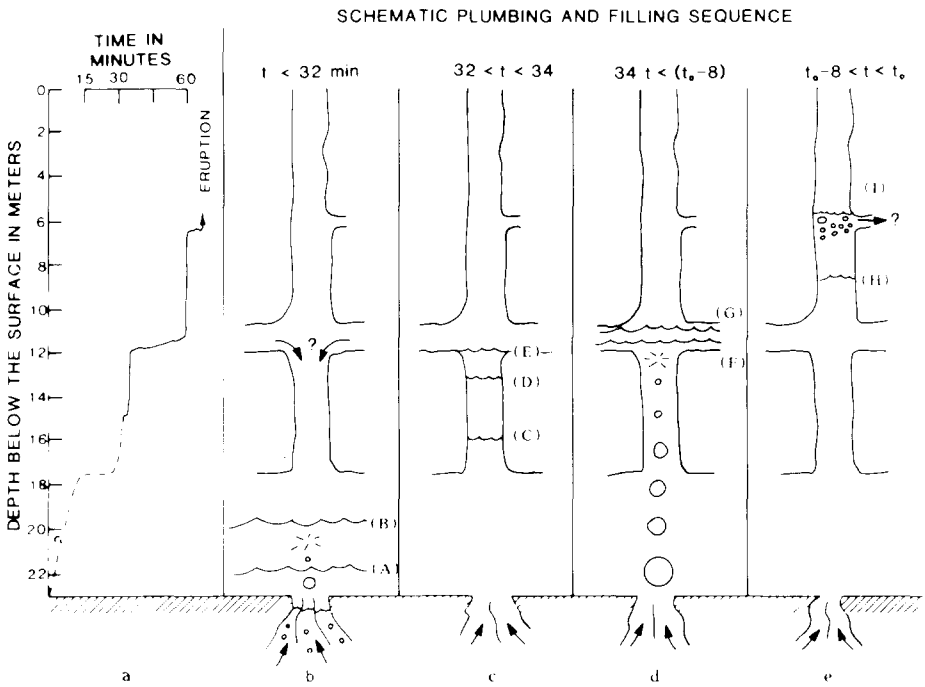

Fig. 5. a. The rate of rise of water in the conduit of Old Faithful, as reported by Birch and Kennedy (1972). b, c, d, and e. Schematic drawings of the simplest geometric configuration of the conduit, or "immediate reservoir" in the terminology of Don White (pers. commun., 1983) that could account for the nonuniform rise rate shown in (a). Consecutive water levels are indicated by A, B, C, D, ... I. Steam bubble formation and collapse indicated schematically by bubble symbols.

The discontinuous rise in water level shown in Fig. 5a was observed in all six monitored intervals and therefore does no appear to be due to random processes (such as formation of big steam bubbles), or to irregularities in water supply rate; rather, it appears to be an intrinsic property of the geyser plumbing system. If the recharge rate is constant (a reasonable assumption for the Old Faithful area because of the drilling conclusions of White et al..

1975), then conservation of mass requires that times of slow rise in level correspond to filling of parts of the conduit of relatively large cross-sectional area, whereas times of rapid rise in level correspond to filling of narrower conduit parts. This is suggested semiquantitatively in Fig. 5b–e. The conduit is envisioned to be a cylinder with possibly two zones of enlarged cross-sectional area: they may be actual zones of storage on the conduit, as shown in the Figure, or may be aquifers or fissures that permit access to storage volumes accessible from these levels. The bottom of the conduit is assumed to be geyserite, with one or more narrow openings that permit recharge of hot fluids from the deeper geothermal system below.

It is important to note that the filling of a channel with irregular cross-sectional area would cause an irregular rise of pressure in water in the system: during times when narrow parts were filling, the hydrostatic pressure at depth would be rising very rapidly, whereas during times when cavities of large cross-sectional area were filling, the pressure at depth would be relatively constant. One result would be that boiling might only occur during the times of filling of the cavities and would be temporarily suppressed by the sudden pressure increase as the narrow conduit parts were filled. This hypothesis and its implications for the seismicity will be discussed in more detail below.

E. Robertson (pers. commun., 1977) has measured the discharge of liquid water from Old Faithful to be approximately 1800 gallons per minute (6.8×10^6 $cm^3 s^{-1}$) during the initial phase of the eruption; because this estimate is made on the basis of flume measurements of runoff water, it does not include an estimate of the steam fraction and is therefore a conservative estimate. To obtain a rough estimate of the recharge rate into the conduit, it is reasonable to assume about 5400 gal (20.4×10^6 cm^3) discharge from a 3-min eruption, followed by a 60-min recharge cycle. Note that this volume of discharge approximately agrees with the volume obtained from the dimensions of the immediate reservoir ($1.6 \times 0{,}6 \times 22 m^3$). This gives a constant recharge rate of 5.7×10^3 $cm^3 s^{-1}$; variations in recharge interval might cause this number to vary between 4.5 and 6.3×10^3 $cm^3 s^{-1}$ (R. Hutchinson, pers. commun., 1983).

Eruption dynamics

Interpretation of the seismic data presented below requires an understanding of the processes that transform relatively cool liquid water in the conduit at the beginning of recharge progressively into hotter water and then into the two-phase liquid–vapor mixture that erupts. The BK thermocouple measurements suggest that immediately before an eruption the fluid in the conduit is liquid water (see Figs. 6 and 12); this is an *assumption*, however, based on the fact that temperatures are well below the reference boiling curve appropriate for hydrostatic pressure of liquid water, but pressure was, in fact, not measured. If there is substantial steam formation within the

water column, the density, and hence the hydrostatic pressure, will be lowered, and the reference boiling curve would be displaced toward lower, and possibly much more irregularly distributed, pressures. In the absence of evidence for large amounts of steam formation continuously throughout the recharge cycle of Old Faithful, the following discussion assumes that the pressure is generally that given by the hydrostatic pressure of liquid water. The eruption dynamics problem is to explain the transformation of the column of liquid water into the two-phase liquid—vapor mixture that is observed to erupt.

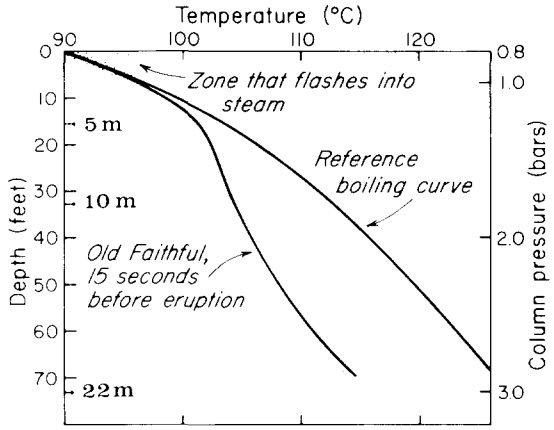

Fig. 6. The temperature in Old Faithful 15 s before eruption compared with the reference boiling curve for a standing column of pure water. Data from Birch and Kennedy (1972).

Convection within the conduit ultimately brings near-surface water close to the boiling curve, where steam can form (Birch and Kennedy, 1972; their data are shown in Fig. 12 which is discussed later in the text). Boiling and/or vigorous ejection occur when the temperature of a near-surface parcel of water intersects reference boiling curve conditions. If only a small amount of water transforms to a two-phase liquid—vapor mixture, and if the overall temperature distribution of the water in the conduit is far from the reference boiling curve, then the only result of such a convective episode is preplay, observed visually as a puff of steam from the vent or a short burst of water and steam. An actual eruption occurs when such a near-surface mass of water boils and is displaced from the conduit if and only if the underlying water is sufficiently close to the boiling curve that the lowering of pressure caused by the initial burst brings deeper water onto the boiling curve.

A semi-schematic illustration of the triggering and the events that immediately follow it is shown in Fig. 7. In each part of this figure, the physical state of the fluid in the conduit is shown on the left, and a space-time diagram of the fluid motion is shown on the right. The initial conditions are as shown in Fig. 7a, where a few meters of water has just flashed to steam and has been unloaded, at a time taken as $t = 0$. After triggering, the surface of

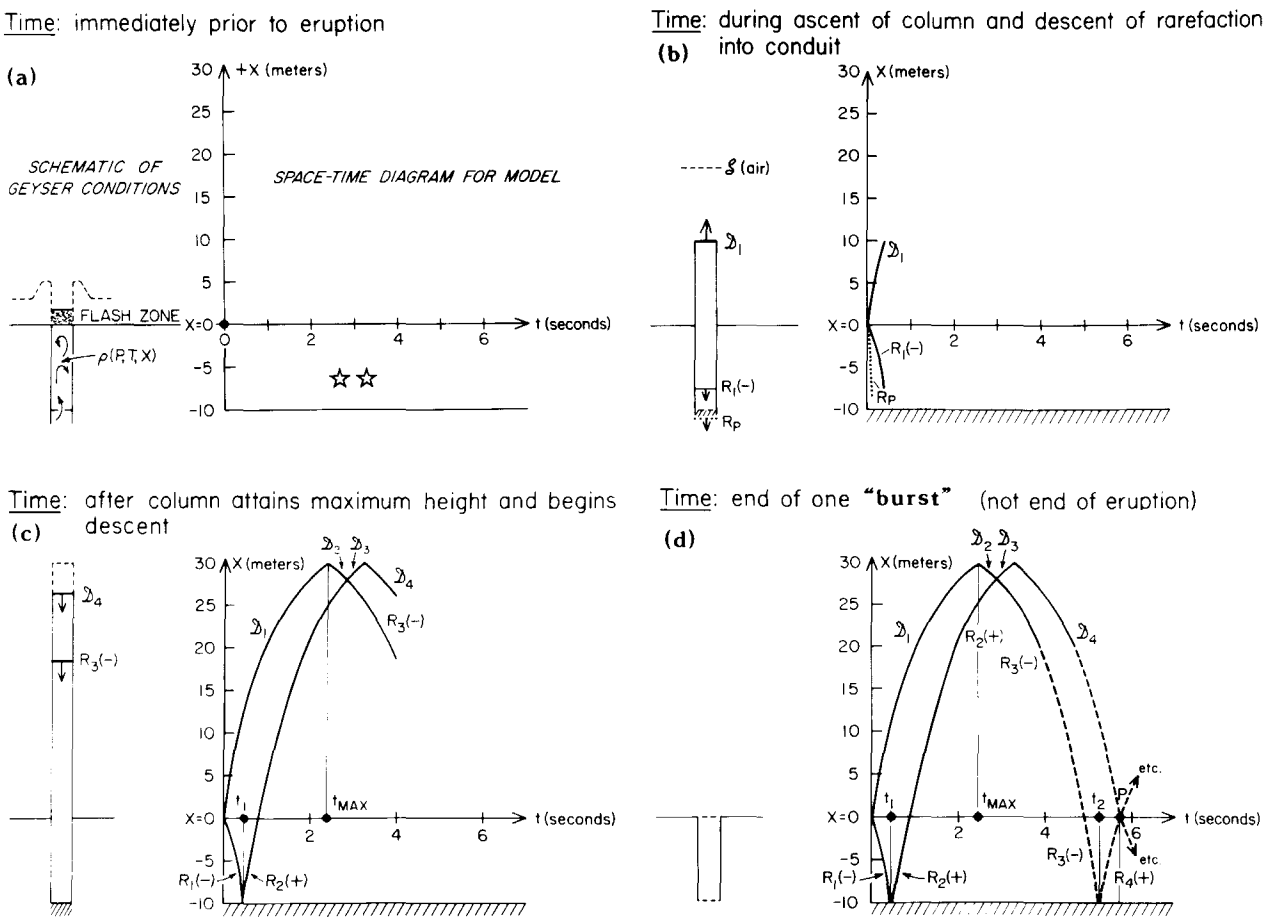

Fig. 7. a, b, c, d. Schematic illustration of the dynamics of the early part of an eruption of Old Faithful, based on Stanyukovich (1960) discussion of gas behavior, and Bennett (1971, 1972, 1974a, b) discussions of vaporization waves. The two stars in the top 10 m of H_2O in (a) indicate that water above the line at 10 m is close enough to the reference boiling curve that it will vaporize upon unloading of the overlying flash zone. See text for discussion of other symbols.

the conduit fluid begins moving upward, as indicated by D_1 in Fig. 7b. This upward motion of the top fluid sends a compression wave (S in Fig. 7b) into the air; this wave is so weak that it is not visually observed at Old Faithful and it is ignored for the rest of the discussion.

At the same time, decompression begins in the fluid remaining in the conduit. Few data exist about the nature of rapid decompression in fluids undergoing vaporization. Two possibilities arise that cannot be distinguished on the basis of data available at this time: (1) The depressurization may occur through supersaturation and sudden nucleation of the vapor phase in water decompressed well below its saturation pressure; or (2) it may occur through a two-step decompression process such as that proposed by Bennett (1971, 1972, 1974a, b). While extensive supersaturation has been observed in laboratory experiments in which superheated water is suddenly exposed to a much lower pressure, the physical conditions at Old Faithful do not lead to sudden large changes of pressure. The pressure change associated with the unloading of a few meters of surface water is rather small (order of 0.1 bar) compared with the pressure change needed at depth to bring the water to the reference boiling curve (nearly 1 bar, see Fig. 6). Consequently, the amount of supersaturation that could be invoked is relatively small, and so supersaturation throughout the fluid column seems to be unlikely. The following interpretation of the eruption dynamics is therefore based on the Bennett vaporization wave theory, with recognition that within each successive vaporization wave discussed below, local supersaturation may also play a role.

Upon unloading of the surface water, a decompression wave, called a *rarefaction* is propagated downward into the liquid water in the conduit; this wave travels at the speed of sound in liquid water, about 1440 m s^{-1}. For reasons that will become apparent, this wave is called a *precursor rarefaction*, shown in Fig. 7b by R_P. The precursor rarefaction carries a certain pressure release, a fraction of a bar for the situation illustrated in Figs. 6 and 7. If the precursor rarefaction travels through water that is sufficiently close to the reference boiling curve (refer to Fig. 6), the pressure decrease may be sufficient to allow some deeper water to reach the local saturation pressure. If, however, the temperature distribution in the water column becomes too far removed from the boiling curve, then the precursor rarefaction does not release the pressure down to the saturation pressure. In such water, the precursor wave travels on downward simply reducing the pressure, but not bringing the water up to the boiling curve. The temperature distribution in the water column after passage of this wave is shown schematically in Fig. 8 as the change from the initial temperature distribution to that on curve 1. The precursor rarefaction traverses the full length of the water column (16 m) in about 0.01 s. It reflects from the silica-sinter surface at the base of the water column and reverberates back and forth as a weak wave trapped in the liquid water.

The precursor rarefaction brings some fluid to the reference boiling curve

(or supersaturates the fluid with respect to its boiling pressure). A second rarefaction, termed a *vaporization wave* (shown as $R_1(-)$ in Fig. 7b) follows the precursor rarefaction through water in this condition and transforms the water into a two-phase liquid—vapor mixture. This wave travels at the speed of sound of the two-phase liquid—vapor mixture, a few to a few tens of meters per second (see Fig. 9) depending on whether equilibrium or non-equilibrium conditions hold (Kieffer, 1977b). In Fig. 7, the vaporization wave velocity has been assumed to be 50 m s^{-1}. The vaporization wave is the working wave that accelerates any fluid that has been brought to the boiling curve by the precursor rarefaction out of the conduit.

The vaporization wave cannot traverse any water that has not been brought to the boiling curve by the precursor rarefaction, so when it encounters liquid water it is reflected back out of the conduit; this wave is shown as $R_2(+)$ in Fig. 7c. In a simple model that does not account for lateral spreading and reflections of the waves in the erupting column, the reflected rarefaction $R_2(+)$, travels up to the top of the erupting column where it is reflected back down the erupting column as $R_3(-)$. If the column were perfectly elastic, if the fluid were behaving like a perfect gas, and if the process were completely reversible, conditions would return to the initial conditions after about 6 s (Fig. 7d). However, in reality, the process is not reversible and part of the erupted fluid falls to the side after stage c on Fig. 7 and the process (b—c) is repeated before completion of the hypothetical cycle (b—d). Each cycle results in removal of some of the fluid and reduction of pressure on the underlying fluid. More and more fluid in the conduit is

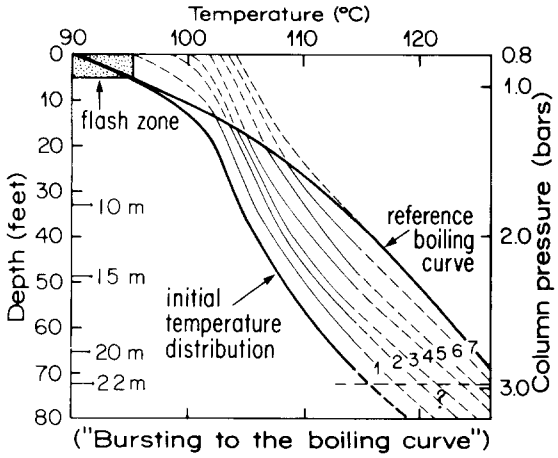

Fig. 8. Illustration of changes in pressure at depth in Old Faithful as successive volumes of water are ejected from the conduit. The depth unloaded each time was chosen so that seven episodes of unloading would take most of the water onto the boiling curve. If the initial temperature distribution at depth is not subparallel to the reference boiling curve, the process may extend on in time past the bursting shown.

transformed into a two-phase mixture as overlying fluid is sequentially erupted because the hydrostatic pressure on the underlying water changes as water vaporizes and erupts. Depending on the initial state of the water in the conduit, many multiples of this process are required to accomplish the total transformation of the water in the conduit to a two-phase mixture (as is shown schematically in Fig. 8). The duration of each individual burst is determined by the vaporization sound speed of the fluid in the conduit and the combined height of the eruption column and the thickness of the incremental layer to be vaporized. The fact that the process of transforming liquid water to a two-phase mixture takes place over roughly 30 s is critical in interpreting the seismicity accompanying the eruption.

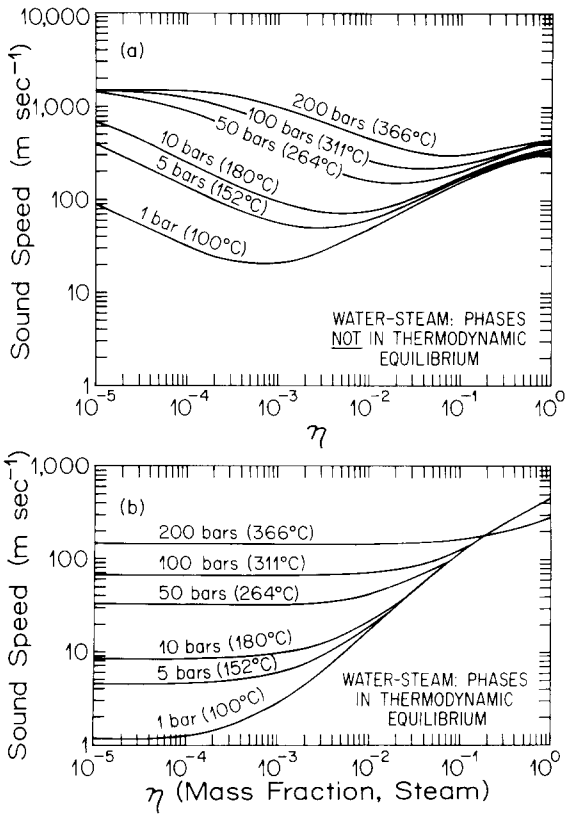

Fig. 9. The variation of the sound speed of liquid—vapor H_2O mixtures (reproduced from Kieffer, 1977b; also see Kieffer and Delany, 1979).

Seismic behavior

The general patterns of seismicity at Old Faithful described below were first reported by Nicholls and Rinehart (1967), Rinehart (1969, 1980), and

Iyer and Hitchcock (1974). In my own study reported here, the seismicity of Old Faithful was recorded on four different seismographs (a Kinemetrics[1]-PS-1A seismic package, loaned by Hiroo Kanamori of California Institute of Technology; Teledyne[1]Portacorders; U.S. Geological Survey smoked drum recorders; and U.S. Geological Survey 5-day magnetic tape recorders), and with a variety of seismometers with natural frequencies of 1 and 2 Hz. Filters having peak responses from 2 to 60 Hz were used; the data presented here for Old Faithful are from the 5-day recorders that had a uniform response to signals between 0.1 and 60 Hz, and a 12 dB/octave roll-off outside of this range. Both vertical and horizontal orientations were used for the seismometers. The seismic behavior described below is for a vertical seismometer placed about 20 m north of Old Faithful. Statistics are given here on signals whose peak-to-peak amplitude exceeds 4 cm s^{-1}.

In general appearance the seismic record of each eruption cycle of Old Faithful looks like the record shown in Fig. 1a and, at higher resolution, in Fig. 10a. The record in Fig. 10a is for an interval of about 76 min duration, following an eruption that occurred near midnight. The duration of the eruption was approximately 4.5 min long, as inferred from equation 1. Histograms of number of events per minute with ground motions in excess of 4 cm s^{-1} for three eruption cycles, including the one shown in Fig. 10a, are shown in Figs. 11 and 12. To work back and forth between Fig. 10a and Fig. 11b, note that time $t = 0$ for Fig. 11b is at approximately 0721 on Fig. 10a. Analysis of about 50 histograms, of which these are representative, suggests that there are 5 phases of seismic activity:

Phase 1: Eruptions (shown at both the beginning and end of the record on Fig. 10a, and, in Fig. 10c) are characterized by a high-frequency wave train ($f \geqslant 40$ Hz) of about one to one-and-a-half minute duraction. There are so few low frequency components in this eruption wave train that when observed with filters peaking at 1—10 Hz the eruption is seismically undetectable (see also the discussion on Lone Star geyser that follows). The eruption wave train is distinctive because: (a) the frequencies are high and relatively narrow-band (spectral analyses have not yet been done because the instruments used to date do not record frequencies over 60 Hz, where there may be appreciable frequency content; new equipment has been designed); (b) the onset is usually gradually emergent, but may contain discrete large-amplitude signals of a few seconds duration; (c) amplitude of the wave train decreases gradually over the one to one-and-a-half minutes that it is detectable. The wave train does *not* last the whole eruption, and there is no seismic indication of the end of an eruption. The detailed shape of the wave train varies from one eruption to another.

Phase 2: The interval following a long eruption begins with a period of

[1] Use of trade names is for identification purposes only and does not constitute endorsement by the U.S. Geological Survey.

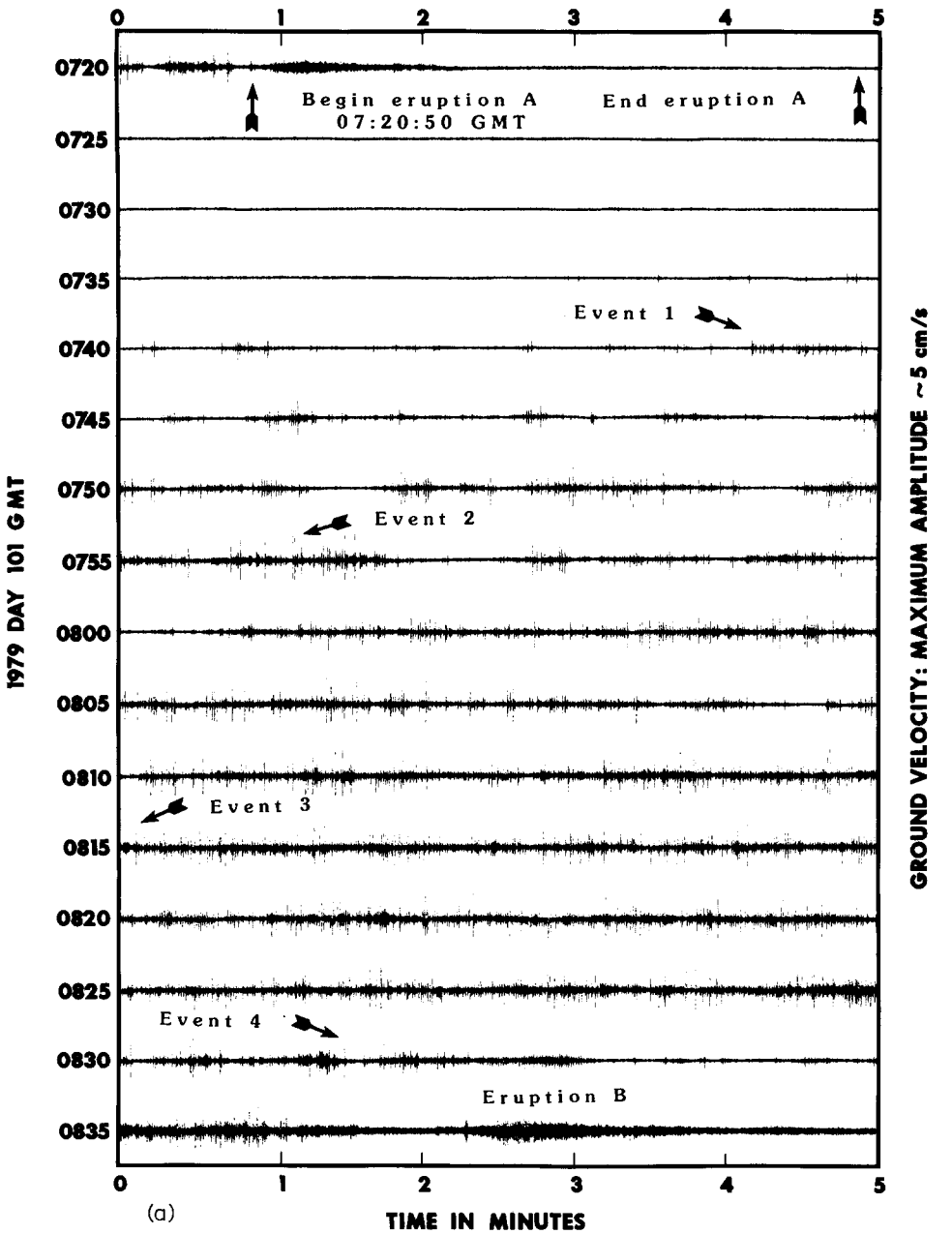

Fig. 10.a. Seismic record of an eruption cycle of Old Faithful. The histogram of the number of events per minute for this eruption cycle is shown in Fig. 11b.

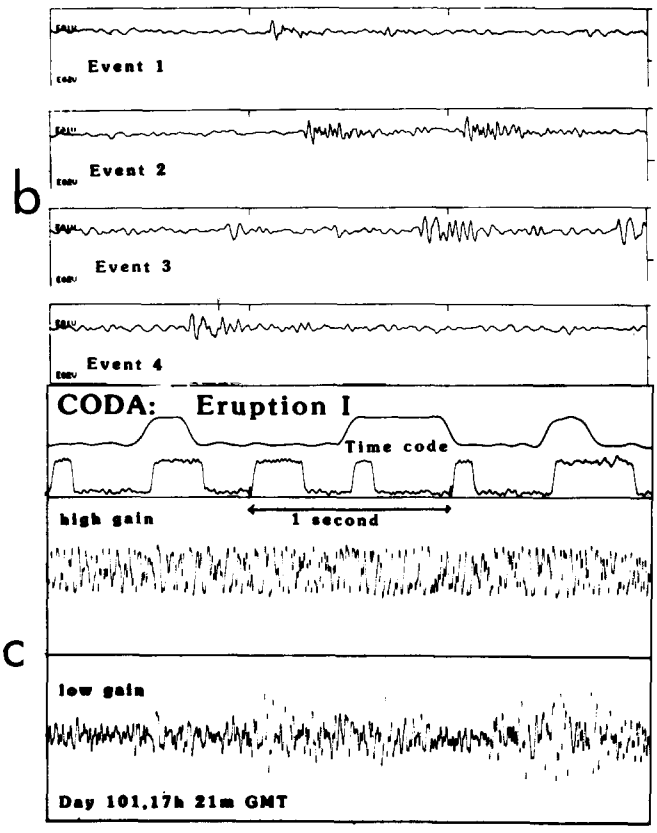

Fig. 10.b. Details of four impulsive seismic events from Old Faithful. The times in eruption cycle of these four events are shown on Figure 11b. c. A detail of an eruption coda for Old Faithful.

no seismic activity lasting about 15 min (from 0725 to 0739 in Fig. 10a; from t = 4 to 18 min in Fig. 11b).

Phase 3: This period of no-activity is followed by a period of low-level seismicity for about 20 minutes (0739—0759 in Fig. 10a; from t = 18 to 38 in Fig. 11b). The seismicity consists of discrete wave packets whose recurrence rate increases in an irregular fashion through the recharge interval. The wave packets typically have frequencies of 10—40 Hz during this time, and their duration is less than ~0.3 s (see Fig. 10b). This period of low-level activity typically terminates with one or two minutes of decreased seismicity (0757 to 0758 and 0800 to 0801 in Fig. 10a; minutes 36 to 37, and 39 to 40 in Fig. 11b).

Phase 4: The low-level activity is followed by a period of about 30 minutes in which the recurrence rate of the wave packets sharply increases toward maximum values of 60 to 80 pulses/minute (0801 to about 0831 in Fig. 10a). This period of high activity typically ends with a minute or more of dramatically decreased seismicity (0833 to 0835 in Fig. 10a; 72—74 min in Fig. 11b).

Phase 5: The seismicity is typically low and erratic in nature for the 5—10 min (sometimes as much as 30 min) preceding an eruption. The overall seismicity generally declines for a few to 10 min before an eruption (from 0831 on in Fig. 10a; from 71 min on in Fig. 11b). A period of several minutes of negligible seismicity often precedes the eruption (from 0836 on in Fig. 10a). I refer to this as the period of *seismic quiet*. Seismic quiet may precede preplay (probably from 0833 to 0835 in Fig. 10a and 72—74 min in Fig. 11c); and seismic noise will resume after a period of preplay (as from 0835 to 0836 in Fig. 10a, and 74—75 minutes in Fig. 11b); multiple episodes of this sequence may precede the actual eruption as the top of the water column boils, erupts briefly and thus is cooled, and reheats.

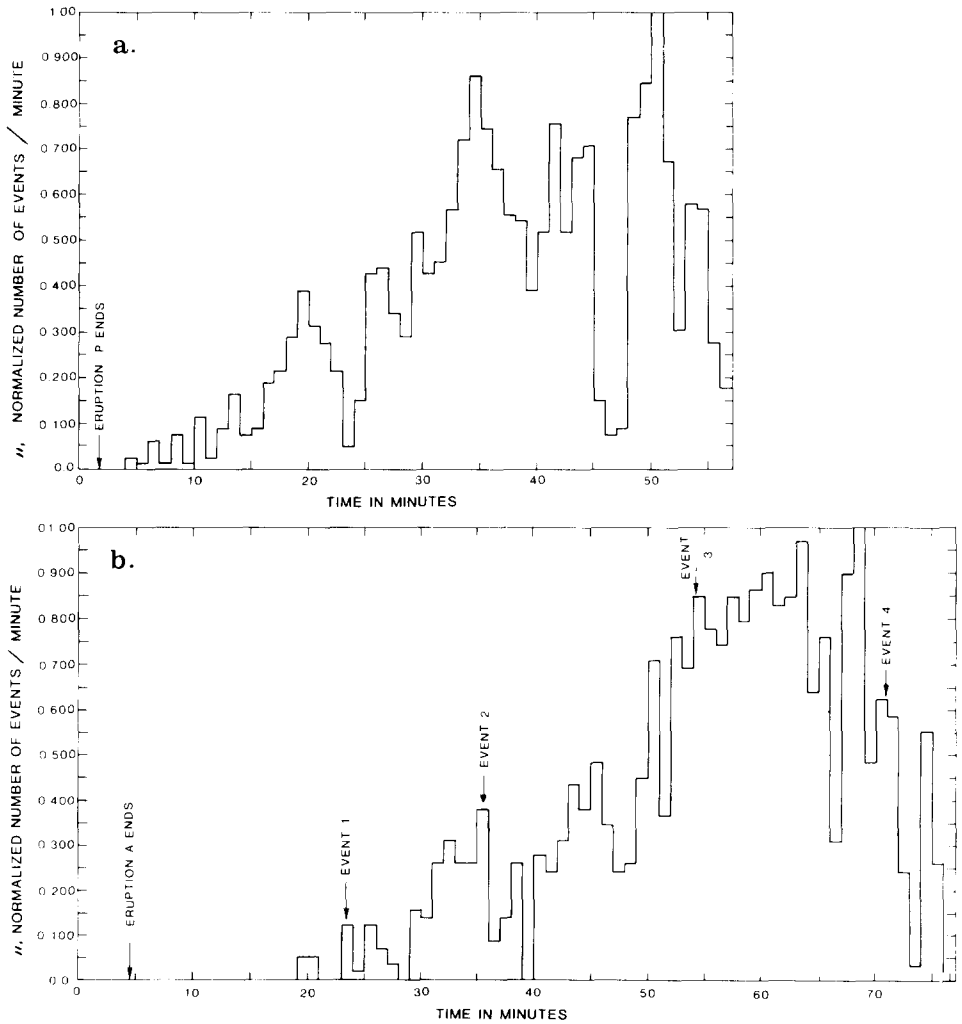

Fig. 11. Histograms showing the number of seismic events per minute through a short (a) and long (b) eruption cycle. In (b), the four events marked are the ones shown in Fig. 10b.

In detail, seismic patterns vary considerably, as shown by the 3 histograms shown in Figs. 11 and 12, but readers are urged to convince themselves that phases 1—5 described above occur in Figs. 11a and 12. The duration of the phases is not always easily defined because there are variations in the recharge history that cause the seismicity, as discussed below, but a study of many eruption cycles has shown that the same sequence generally occurs. Curves of cumulative number of seismic events vs. time into the interval show the same information as the histograms in a much more compact way; cumulative curves for 23 consecutive eruptions are shown in Fig. 13, and phases 1—5 described above can be identified on each by changes in slope of the curves. Periods of low-level seismicity are the parts of the curves with the shallowest slopes. These curves reveal that seismicity resumes quickly after a

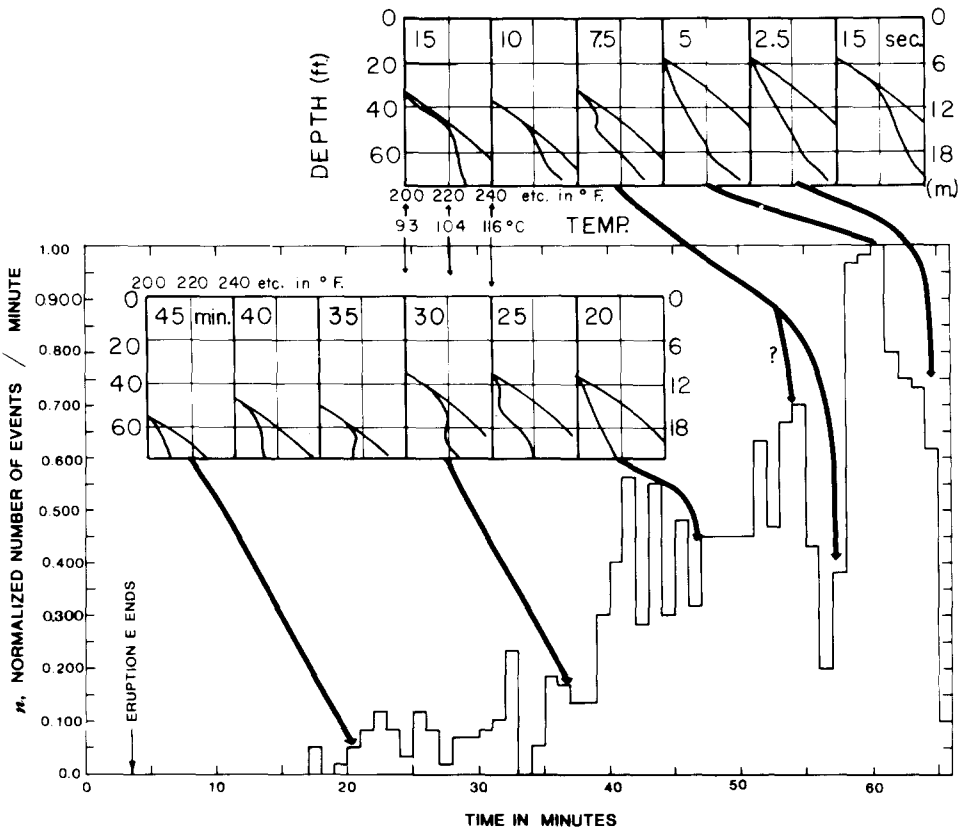

Fig. 12. Histogram of the number of seismic events per minute through a medium length interval that closely corresponds to the length of interval in which the Birch and Kennedy thermocouple and float data were taken in 1948. The temperature-depth-time curves measured by Birch and Kennedy (as reported in their 1972 paper) are shown, and arrows are placed to indicate approximate correlations with seismic behavior. The correlations were made by simply subtracting the Birch and Kennedy times before eruption from the 66-min interval on the histogram. Times before the next eruption are given in minutes.

short eruption: for the four short eruptions included in this study, the seismicity resumed within 4—7 min after the previous eruption had started. After a long eruption the time to resumption of seismicity varies between 18 and 30 min (see Fig. 12), in most cases it resumes within 21±3 min.

The curves of cumulative number of seismic events also reveal that the length of the interval between eruptions is *not* directly related to the total number of events (see histograms), nor to the maximum number/minute that occur (not shown), nor to the time required for resumption of seismicity after an eruption (Fig. 13). Short and long intervals can show either a

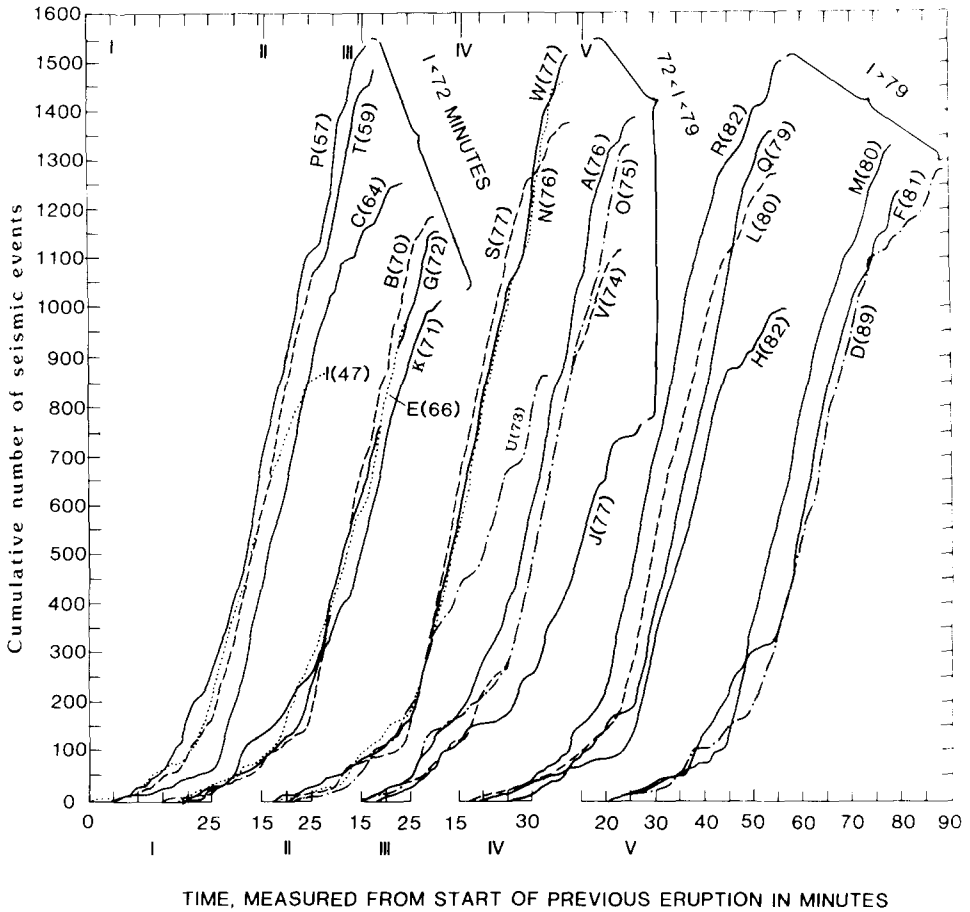

Fig. 13. Cumulative curves of the number of seismic events through 23 consecutive eruption cycles. The seismometer was in the same place for all eruption cycles. The events occurred in the order A, B, C ... For conciseness and clarity, groups of eruptions, labelled I, II, III, IV, and V have been offset along the bottom axis, with the 15-min mark displaced. Lines of different weight or symbols are used only for clarity. Numbers in parentheses indicate the length of the interval. The overall similarity of the curves shows that the gross features of eruption cycles are repeated; the fine differences in slopes, total number of events, etc. show that there are also significant variations in recharge behavior.

relatively small cumulative number of events (about 800) or a relatively large number (about 1500). Neither the histograms nor the cumulative curves have revealed any indicator whether an imminent eruption will be long or short.

All of the large amplitude seismicity appears to be caused by processes in the immediate reservoir, since it coincides with the measurable filling of that section. Therefore, it appears that the variations in conditions that give rise to short vs. long eruptions are below or outside of the 22-m-deep immediate reservoir, and that for both long and short eruptions conditions in the immediate reservoir are similar at the onset of the eruption. This is consistent with the observations of Rinehart (1980) and analysis of movies of the eruptions (Kieffer, unpubl. data, 1983) that the visible eruption play during short eruptions is similar to the play during the first 3 min of long eruptions. The differences occur only in the late-stage prolonged low-level emission of hot water in long eruptions.

Correlation of seismic behavior with data on the eruption cycle

With proper care taken to account for the fact that each eruption cycle is unique in detail, data sets taken at different times can be correlated because Old Faithful has maintained a remarkably uniform general pattern for over a century. Hence, it is assumed that in a general way the BK temperature-depth-time curves are relevant to the current conditions in Old Faithful and, hence, to the seismicity. The temperature-time curves are superposed on a histogram for a 66-min interval in Fig. 12. Although the conclusions that can be drawn by piecing together such disparate data sets cannot be as firm as those that would be obtained by applying all observational techniques simultaneously, the data do suggest the following relations between the seismicity and recharge cycle:

(1) During the first 21±3 min of a long interval when there is no seismicity, the water level in the conduit is below 18 m.

(2) During the 25-min period of low-level sesimicity, the water level is at the approximately 18 m depth, and varies up and down by about 3 m due to intermittent boiling. Convective overturn of water with presumed surface boiling can occur this early in the eruption cycle.

(3) The 30-min period during which the seismicity rises rapidly toward the maximum recurrence rate occurs while the water is at about the 11—12 m level.

(4) The brief period of no seismicity that separates the periods of low- and high-level seismicity (2 and 3 above, respectively) appears to correspond to the time when the water rises from the 18 to the 11 m level, and another period of low seismicity appears to correspond to the time when the water rises from 11 m to 6 m.

(5) During the last 10 min of the recharge cycle, the water level rises to about 6 m depth. During this time, the seismicity generally declines, and may cease entirely for periods of tens of seconds to even a few minutes prior to preplay or eruptions.

COMPARISON OF THE SEISMICITY OF OLD FAITHFUL WITH OTHER GEYSERS

Interpretation of the seismic data of Old Faithful benefits from comparison of its seismic and recharge patterns with those of other geysers where additional visual observations are possible. Broadly speaking, there are two classes of geysers: *columnar geysers*, of which Old Faithful is an excellent example, and *fountain geysers*. Columnar geysers have narrow vertical or subvertical columns of ejected water and steam, they generally do not have a surface pool and, consequently, there is little direct surface recharge into their conduits during the course of an eruption. In contrast, fountain geysers usually have surface pools of water and are characterized by ejections of water from the vent as major bubbles of steam rise through the vent into the surface pool. The ejections are intermittent throughout the duration of the eruption. The ejection is through a relatively large range of solid angle, so that the eruptions are casually described as "sloppy." Because the large surface pools collect ejected water that drains back into the conduit, abundant liquid is available during the eruption of a fountain geyser. The eruptions usually terminate while there is still liquid water in the system because heat is exhausted from the plumbing system and the eruption is "quenched" by water that has cooled by ejection.

As reported by Nicholls and Rinehart (1967), seismic signatures vary from one geyser to another. Typically there is a high level of background noise prior to eruption; for example, Iyer and Hitchcock (1974) reported that background noise levels away from the geyser basins in Yellowstone were on the order of $14—28 \times 10^{-3}$ $\mu m/s^{-1}$, whereas the rms amplitude near Old Faithful rose as high as 3 $\mu m\ s^{-1}$. Superimposed on the background noise may be impulsive seismic signals whose recurrence rate increases as an eruption approaches. The wave packets of the impulsive signals have a variety of characteristic shapes, which are generally unique to a particular geyser and its environment. The seismic signals are of high amplitude (typically, velocities of 1—10 cm s^{-1} are recorded near the vent, $10^3—10^5$ times background level at nongeothermal areas), and have very high, generally monochromatic, frequencies (dominant frequencies above 5 Hz).

During eruptions of fountain geysers, seismic signals characteristic of the pre-eruption phase continue at approximately the pre-eruption amplitude and frequency. A typical seismic record from an eruption of Narcissus geyser is shown in Fig. 14. In a Narcissus eruption, water is thrown into the air in a series of discrete bursts. Movie films taken simultaneously with the seismic tracings demonstrate that the seismicity is generated by ground response to (a) individual bubbles bursting and splashing in the surface pool, and (b) bubbles collapsing before reaching the surface. Relations between seismic activity and surface eruption play are similar at Grand and Pink geysers in Yellowstone and at Strokkur (Fig. 15) in Iceland.

At Strokkur, pre-eruption seismic signals are frequently associated with audible "thumps" and the temporary formation of "water hills", both taken

to indicate the formation and collapse of steam bubbles in the underground reservoir or conduit. An eruption consists of one to five bursts of a 2-m bubble of steam through a surface pool of water. The bursts are separated by 10—20 s. Asymmetric breakout of steam through the bubble wall, or nearly-simultaneous emergence of multiple bubbles can complicate the bursts. In the summer of 1982, the intervals between eruptions of Strokkur were following a rule rather similar to that of Old Faithful's intervals:

$$I = 0.5 + 2.5\,n \qquad (2)$$

where I is the interval lenght in minutes, and n is the number of bursts in the preceding eruption. This equation was good to within ± 1 min.

The seismic signal associated with each burst during a Strokkur eruption is brief, and ceases even before the pool refills with water (Fig. 15). About 20 s after the last burst, the seismicity resumes, sometimes accompanied by audible thumping. As suggested by Rinehart (1980), this post-eruption seismicity seems likely to be due to the temporary formation of steam in under-

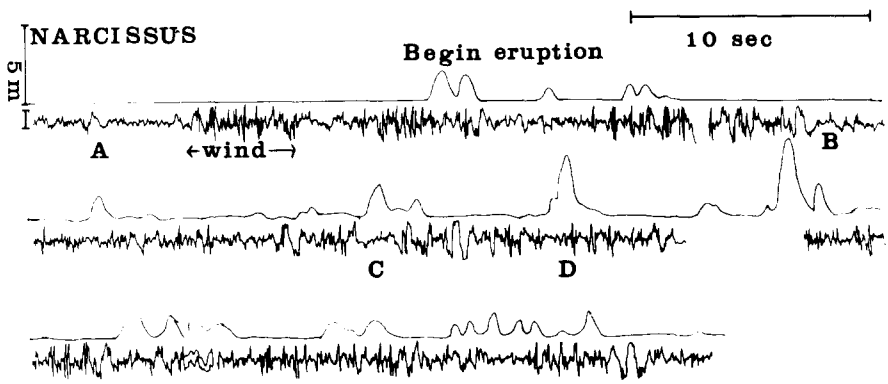

Fig. 14. A comparison of seismicity with eruption play for a typical fountain geyser, Narcissus, in Yellowstone. The bottom line of each pair is a tracing of a seismic record taken concurrently with movie films. The top line of each pair shows the height of the play measured from the films. A, typical pre-eruptive activity; B, ambient pre-eruption noise continuing between bursts; C, D eruptive bursts. The eruption continued long after the section shown here.

Fig. 15. Seismic record from Strokkur Geyser in Iceland, showing seismicity as two bursts occurred (labelled E), and the post eruption coda (labelled R), assumed associated with recharge into underground cavities. The small timing marks under the asterisks are 20 s apart.

ground cavities as the system begins recharging, and collapse of these steam bubbles as they interact with cold water pouring into the system at this time.

In summary, in spite of their individual differences, fountain geysers appear to have in common a high level of background noise. Impulsive signals can be attributed to the explosion, implosion, or sometimes more complicated motion, of individual bubbles immersed in, or travelling through, liquid water.

In contrast to the fountain geysers where the seismicity accompanies the distinct bursts and retains the character of the pre-eruption signals, at columnar geysers the seismicity characteristic of the pre-eruption phases significantly decreases or disappears and is usually replaced by an eruption coda of appreciably different character, as was discussed in detail above for Old Faithful. The decrease or disappearance of the pre-eruption seismicity may occur significantly prior to surface play (as, in the case of Old Faithful where the signals decrease as much as 4 min prior to eruption), or gradually, at the start of an eruption as described below for Lone Star. At Old Faithful, the background level of noise stays high (see the thickening of the main trace in Fig. 10a as time increases toward the eruption on the bottom line), but the number of impulsive events dramatically decreases.

At Old Faithful, the decrease in impulsive events is masked during the first minute of the eruption by the high-frequency wave train, but Figs. 10a and 1b, as well as other observations made with narrow band pass filters, show that the impulsive signals are clearly absent in the later part of eruption. The eruption wave train at Old Faithful is sustained harmonic tremor at a frequency comparable to, or somewhat higher than, the frequency of the unsustained preeruption events. Similar wave trains occur at during eruption of other geysers that have columnar characteristics (e.g., Beehive, shown in Fig. 16; Daisy; Great Geyser during some phases of its large eruptions).

Considerable insight into the seismicity of columnar geysers can be gained by an examination of the record from Lone Star geyser. When Lone Star is

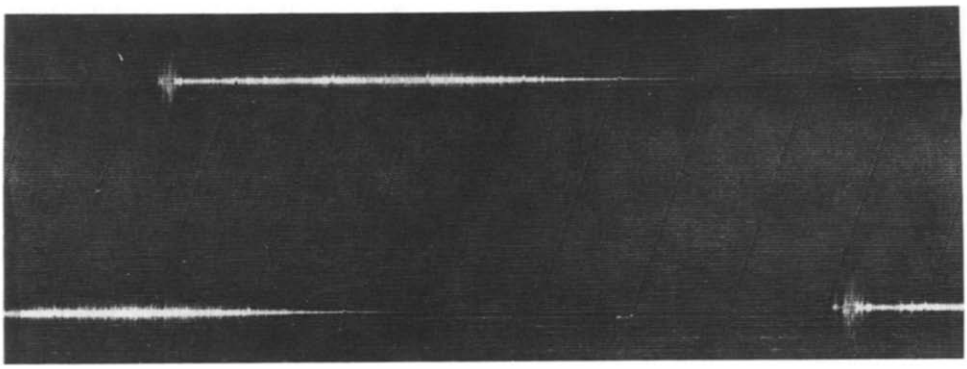

Fig. 16. Two seismic codas of Beehive Geyser, Yellowstone. The timing marks are one minute apart. The second eruption begins on the right side and wraps around to a lower line appearing on the left.

observed with broad-band high-frequency instruments, it shows a wave train similar to Beehives. However, when it is observed with narrow-band, low-frequency instruments, there is no eruption wave train (Fig. 17). The onset of a Lone Star eruption is not well defined, because the geyser boils and plays to heights of more than 3 m intermittently for as much as 1 hr before the actual eruption. During this time, the seismicity much resembles the seismicity of splashing fountain geysers, as shown by the samples in lines 1–10 of Fig. 17. However, as the preplay becomes more vigorous and continuous, the seismicity decreases. Line 11 of Fig. 17 was recorded just a few seconds before a vigorous surface preplay episode; not the extreme quiet (which may have been going on for several minutes before the seismometer was turned back on) in comparison to earlier noise. The geyser remained seismically quiet for 1 min (line 11) and the arrival of discrete pulses interpreted as p-waves signalled the resumption of seismic noise. As the preplay continued, the discrete pulses merged into continuous noise (lines 12 and 13). The noise declined continuously over about 3 min (lines 13—15), and at the time of the onset of seismic quiet in line 15, the geyser attained its maximum height. It continued to play for about 20 min and the seismic record was so quiet that we occasionally stomped on the ground to make sure that the recording

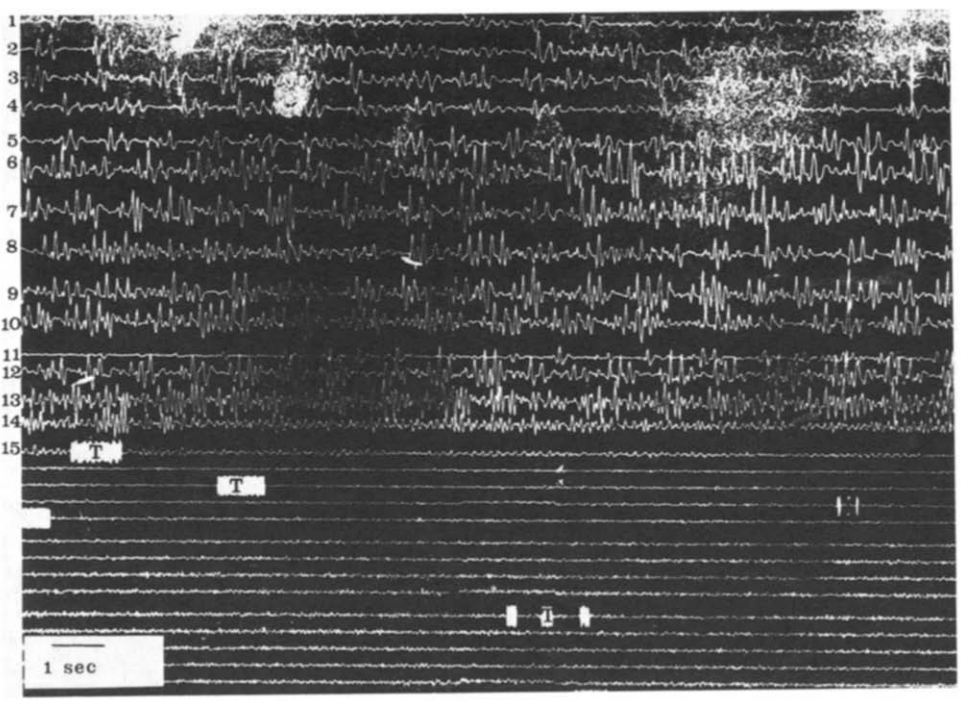

Fig. 17. A seismic record from Lone Star Geyser, Yellowstone National Park, U.S.A. This photograph shows about half of the total width of the tracing. Lines 1—10 represent samples of the seismic noise for 1/2 hr before the eruption, each pair of lines being a 1-min sample out of a 5-min interval. The seismometer was on continuously from line 11 on. The areas marked T were test pulses and timing marks.

system had not failed, as on the right side of line 18. After the eruption ceased, the geyser remained seismically quiet, apparently because the conduit was drained of fluid.

In summary, observations at a number of geysers strongly suggest that: (1) strong seismic signals are generated by bubble collapse and/or bubble explosions in liquid water; (2) seismicity retains the pre-eruption character of bubble-related events at fountain geysers; but (3) the nature of seismicity changes from individual events into continuous wave trains at columnar geysers. In addition, studies have also shown that the frequency content of geyser seismicity changes quite markedly over an eruption cycle and that very broadband instruments (1—100 Hz) may be required to fully monitor the seismicity.

RELATIONS BETWEEN SEISMICITY AND ERUPTION CYCLE AT OLD FAITHFUL

A model of seismicity at Old Faithful must:

(1) be consistent with principles of geyser activity as known in general (White, 1967; Rinehart, 1980), and as applied to Old Faithful in particular (Rinehart, 1969, 1974, 1980; Kieffer, 1975, 1977a, 1982; Kieffer and Ihnen, 1977)

(2) address the changing physical properties of the fluid as liquid water transforms to a two-phase mixture of liquid plus vapor (Kieffer, 1977b; Kieffer and Delany, 1979);

(3) account for seismic signals at 20—50 Hz and their absence at lower frequencies;

(4) explain why damping of signals in times on the order of a few tenths of a second occurs during recharge in contrast to the continuous nature of the eruption wave train; and

(5) explain why eruption wave trains last only one to one-and-a-half minutes whereas eruptions last from one-and-a-half to five minutes.

The explanation of seismicity at Old Faithful which follows assumes that all seismic activity is associated with the fluid column. There is no evidence that rock fracturing is important during eruption cycles. It is also assumed that H_2O is the only important component of the fluid in the geyser conduit, i.e., noncondensible gases such as CO_2 and SO_2 are not important. This is a good assumption for Old Faithful, but not for many other geysers in the Yellowstone area.

Pre-eruption seismicity

An obvious source of seismic noise is collapse of transient steam bubbles in the water column. Bubble collapse occurs because gradients of pressure and temperature that develop as the system recharges allow bubbles to migrate from conditions where they are stable into water of different thermodynamic properties. Heat is supplied both by conduction through wall rocks

and the admixture of very hot waters. At Old Faithful, the hot waters are believed to originate in a reservoir at a temperature of ~217°C (Fournier et al., 1976) and to migrate into the conduit near the base of the open reservoir (see Fig. 5); there it enters either as high-pressure water or as steam (White et al., 1975). However, cool water infiltrates the system through high-level aquifers and fissures, and the surface of the water column is continuously cooled by evaporation and conduction. Thus, the water column develops a strong temperature gradient from base to top. Steam bubbles that form at the base condense when they rise into cooler water higher in the conduit. Whereas the growth of a bubble is a relatively slow and, hence, aseismic process, the collapse of a vapor bubble into a liquid of its own composition is very rapid (millisecond time scale). Pressures within the collapsing cavity can be as large as tens to hundreds of kilobars (Fujikawa and Akamatsu, 1978). Because of the small size of a high-pressure collapsed cavity, the transient pressures generated in the vicinity of collapse decay quickly with distance, becoming seismic level disturbances at distances outside a few bubble radii.

A bubble collapse causes waves within the fluid column, as illustrated in Fig. 18a. For simplicity, assume that the bubble collapses in standing water contained in a simple pipe, bounded on the sides and bottom by rigid geyserite. Assume that bubble collapse is instantaneous and, for convenience of illustration, that the collapse occurs at the base of the water column. Let the region of collapse in which the waves are generated be small enough that the waves are acoustic waves throughout most of the column. Consider a simple compression wave or weak shock, C_1, that propagates from the point of collapse outward (Fig. 18b) (the same argument holds if one assumes that the first wave generated is a tensile wave). This wave travels to the free surface

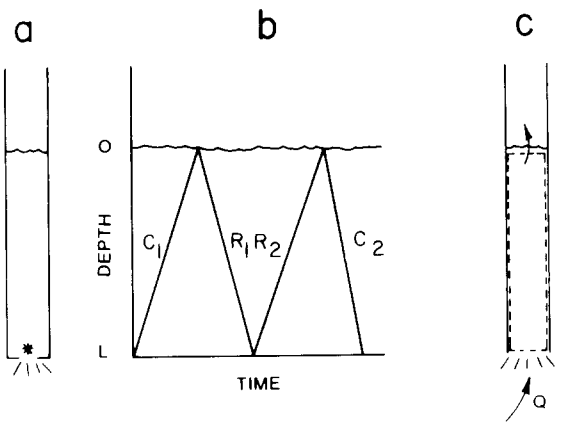

Fig. 18. a. Schematic drawing of waves propagating in a standing column of water of depth L. A bubble collapse at the base of the column is indicated by an asterisk. b. One cycle of waves due to the bubble collapse in the bottom of the conduit. c. Illustration of the notation used for hydraulic transient theory when there is a flux of fluid through the conduit.

of the water at approximately the ambient sound speed, a. The boundary condition at the free surface is that the pressure is constant. The incident compression wave is therefore reflected as an expansion or rarefaction wave, R_1. R_1 travels back through the water column to the bottom of the conduit. Here the boundary condition is that the velocity is zero. Therefore, the rarefaction reflects off of the bottom as a wave of like sign, a second rarefaction wave, R_2. This rarefaction travels to the free surface where it reflects as a compression, C_2. When C_2 reaches the bottom of the conduit conditions are again as they were immediately after bubble collapse and one full cycle has been completed. The period for one complete cycle, T, is:

$$T = 4L/a \tag{3a}$$

or the frequency, f is:

$$f = a/4L \tag{3b}$$

where L is the conduit length and a is the speed of sound in the conduit fluid. A more rigorous treatment would show that the fluid sound speed should be modified to account for the distensibility of the conduit walls (St. Lawrence and Qamar, 1979):

$$a = \frac{(K/\rho)^{1/2}}{[1 + (2K/E)(1 + \nu)]^{1/2}} \tag{4}$$

Here K is the bulk modulus of the fluid, ρ is the density of the fluid, E is the elastic modulus of the conduit, and ν is Poisson's ratio for the conduit material (geyserite, sinter, or sintered deposits). For a conduit of geyserite (assumed to have the bulk modulus and Poisson's ratio of opal) containing liquid water, K = 14.4 kbar, ρ = 1 g cm^{-3}, E = 380 kbar (Birch, 1966, p. 166), and ν = 0.06. Therefore, the modified sound speed is 1385 m s^{-1}, in contrast to the speed of sound of liquid water, 1440 m s^{-1}. Typical values of L, through the times in the eruption cycle when there is appreciable seismicity (phases 3 and 4 described in an earlier section) range from 8 to 16 m. The corresponding frequencies are 43 and 20 Hz, values that approximately span the range of observed frequencies during the recharge interval. Although higher frequency resonances will be present, e.g., the radial modes of oscillation, the frequencies calculated here should be dominant.

In order to calculate the damping of the signals caused by the bubble collapse, it is necesssary to recognize that the water column is not static but rather, is constantly being fed by the recharge water (Figure 18c). Pressure or mass flux perturbations within a system that is flowing can be amplified to resonance as standing waves, known as *hydraulic transients*. The characteristic resonance frequencies of a system and their damping characteristics depend on the relative values of two parameters:

(1) the *characteristic impedance* of the system, Z_c, which, for a frictionless system is;

$$Z_c = a/gA \tag{5}$$

(a is the sound speed, g is the acceleration of gravity, and A is the cross-sectional area); and

(2) the *hydraulic impedance*, Z_h, which, for a simple pipe from a reservoir is:

$$Z_h = 2L/Q \tag{6}$$

(L is the height of the column of water, sometimes called the pressure head, and Q is the volume flux.)

If the hydraulic impedance is greater than the characteristic impedance, the system resonates like a closed organ pipe, with characteristic frequencies:

$$f = \frac{n\,a}{4\,L}\,,\ n = 1,3,5,.... \tag{7}$$

and damping constant:

$$\sigma = \frac{a}{2L}\ln\left[\frac{Z_h - Z_c}{Z_h + Z_c}\right] \tag{8}$$

The approximation discussed above and illustrated in Fig. 18a, b is an end-member of this type.

If the characteristic impedance is greater than the hydraulic impedance, the system resonates like an open organ pipe with characteristic frequencies:

$$f = \frac{n\,a}{4\,L}\,,\ n = 2,4,6,... \tag{9}$$

and damping constant:

$$\sigma = \frac{a}{2L}\ln\left[\frac{Z_c - Z_h}{Z_c + Z_h}\right] \tag{10}$$

For Old Faithful in the preeruption state, Q was estimated at 5.7×10^3 $cm^3\ s^{-1}$. With L taken as 800 cm—1600 cm, the sound speed (modified for distensibility) as 1.385×10^5 cm s^{-1}, and the cross-sectional area as 10^4 cm^2, Z_c is 1.4×10^{-2} s cm^{-2}, and Z_h is 0.28 to 0.56.

Since Z_h is greater than Z_c the water column resembles a standing closed ended pipe, and the fundamental resonant frequency is $f = a/4L$ as calculated above for Fig. 18b. For the range of lengths cited, the damping constant is between −8.6 and −2.2. The characteristic damping time is the inverse of this, or 0.12 to 0.46 s, in good agreement with the observed length of the pulses, see Fig. 10b.

These results strongly suggest that the preeruption seismicity at Old Faithful is due to hydraulic transients in a slowly recharging water column. Preliminary analysis suggests that the frequency of the wave packets decreases from 40 to 45 Hz at the beginning of seismicity down to about 20 Hz at the end of the recharge cycle. This change is in the direction expected due to the lengthening water column. Rigorous application of the hydraulic transient

theory beyond these preliminary calculations must await seismic studies with recorders that have a higher frequency response than those used to date, and must be coordinated with simultaneous measurements of water level in the conduit because the variations suggested by the Birch and Kennedy data are sufficient to allow a rather wide range in frequency content and in damping times of the signals.

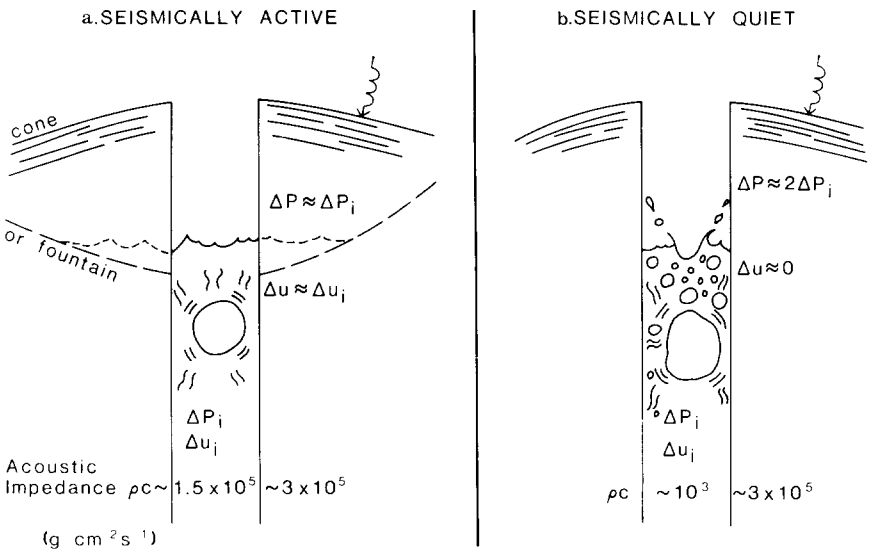

Fig. 19. A schematic illustration of conditions in a seismically active geyser conduit (a) and a seismically quiet conduit (b). The seismically active geyser could be either a fountain geyser (as is indicated by the dashed lines) or a columnar geyser (as indicated by the solid lines) during a seismically active time when the conduit contains liquid water. The seismometer placement on geyserite is indicated by a spring and arrow. Pressure and velocity perturbations of a growing, collapsing or moving vapor bubble are indicated by ΔP_i and Δu_i, respectively. The acoustic impedances of the water, water-vapor mixture, and geyserite are shown on the bottom of the figures.

The hydraulic transients generated prior to eruption are not directly monitored by seismometers, because they are generated within the water in the conduit, whereas the seismometers are located on geyserite near and above the conduit walls (see sketches, Fig. 19). However, when the conduit contains *liquid* water (see Fig. 19a), the hydraulic transients are effectively transmitted to the walls because the acoustic impedances of liquid water and geyserite are very similar. Thus, the "contact" between the water and walls is good. For example, for a simple tensile or compressional wave hitting the wall at normal incidence, the wave velocity u_f and pressure P_f in the region between reflected and transmitted waves are:

$$u_f = \frac{2R_1}{R_1 + R_2} \, u_i \qquad (11a)$$

$$P_f = \frac{2R_2}{R_1 + R_2} P_i \qquad (11b)$$

where $R = \rho c$, subscript 1 refers to the fluid in the conduit, subscript 2 refers to the geyserite, and P_i and u_i are the pressure and velocity in the incident wave (Thompson, 1972). For liquid water, $\rho c \sim 1.5 \times 10.5$ g cm^{-2} s^{-1}, and for geyserite $\rho c \sim 3 \times 10^5$ g cm^{-2} s^{-1}, so the final velocity is 1/3 that of the initial velocity and the final pressure is 2/3 that of the initial pressure (attenuation ignored). The walls can thus be effectively "hammered" by the activity of individual bubbles, and a seismometer placed upon adjacent geyserite will record most of the fluid activity.

Cause of the seismic quiet

As described earlier, Old Faithful has four periods when the seismicity deviates from the general trend of increasing activity through the interval. The causes of each time of reduced activity are different:

Phase 2: After a long eruption, there is no seismic activity for about 21∓4 min because there is no water in the immediate reservoir.

End of Phase 3: There is about one minute of no seismicity separating the initial 20-min interval of low-seismicity (phase 3) from the more intense seismicity (phase 4) that develops. The data in Fig. 11b suggest that this minute is when the water rises rather suddenly from a depth of 17 m to about 11 m.

End of Phase 4: A similar period of decreased seismicity appears to accompany the rise of water from 10 m to 6 m. At the end of phases 3 and 4, decreased seismicity may result from suppression of steam bubble formation at the base of the water column because of the hydrostatic pressure increase accompanying the sudden water rise.

Phase 5: During the last period of seismicity, about 10 minutes before eruption, periods of seismic quiet seem to coincide with times when the top water in the geyser column begins to boil continuously, where the onset of boiling has been documented audibly at close range and visually when it is accompanied by occasional splashes of water and increased steam emission from the vent. [In contrast, there is no correlation of the individual seismic pulses during recharge with increases in steam emission (J. Rinehart, pers. commun., 1983)]. Depending on the total condition of the water column, surface boiling may be followed by either preplay or a full eruption.

The fact that the seismic quiet of phase 5 accompanies preplay as well as actual eruptions is significant. At Old Faithful, preplay ejects water intermittently to heights as great as 3—6 m above the ground surface, perhaps as much as 9—12 m above the actual fluid level in the conduit. Although preplay generally results from sudden convection of hotter water from depth to the surface, the actual play itself involves only the top part of the water column because it is of short duration. Therefore, the association of periods

of seismic quiet with preplay, as well as with actual eruptions, indicates that the phenomenon of seismic quiet of phase 5 results from changes in conduit conditions at fairly high levels — perhaps in the top few meters.

Late in the recharge cycle, steam bubbles that have formed at depth can rise further before collapsing than early in the recharge cycle because the water column is, on the average, hotter (see Fig. 12). Eventually the near-surface waters begin boiling and the migrating steam bubbles can rise into the boiling zone at the top of the conduit. Here, the pressure oscillations induced by their motion (be it growth, coalescence, collapse, or breaking at the surface) cannot be easily propagated either into the walls or into the liquid water underlying the boiling zone because the bubble activity is taking place in a zone of greatly reduced acoustic impedance and increased attentuation (see Fig. 19b). The boiling two-phase fluid has approximately the density of liquid water, but the speed of sound in the fluid is greatly reduced (to as low as 1—50 m s^{-1}) because the vapor is highly compressible and heat and mass transfer between the vapor and liquid phases slows the acoustic waves (Fig. 9) (Kieffer, 1977b; Kieffer and Delany, 1979). Hence, the acoustic impedance is about two orders of magnitude lower than that of the wall rock or underlying liquid water (Figure 19b). Because of the impedance mismatch (see eqs. 11a and 11b), velocity oscillations induced in the boiling fluid by bubble activity cannot be transmitted to the rock or the seismometer ($u_f \approx 0$). An important concept here is that for the fluid to be considered "two-phase" and to have a reduced sound speed, bubbles must be uniformly dispersed throughout (Kieffer, 1977); a liquid with a few bubbles rising through it may not qualify as "two-phase" for calculation of acoustic velocity.

According to these considerations, the period of gradually declining seismicity in phase 5 prior to eruptions is the time when more and more bubbles rise through hotter and hotter water toward the surface without bursting within the column of liquid water. The periods of seismic quiet superimposed on this decline are times when surface boiling masks most bubble collapses or explosions.

The eruption wave train

At the onset of an eruption, *liquid* water is present in the conduit and remains there in decreasing amounts for an appreciable time after initiation of the eruption. Pressure perturbations are generated continuously at the surface by the unloading process (see Figs. 7a, b, c, d). Thus, hydraulic transients within liquid water awaiting eruption are a likely source of the eruption tremor. The model of hydraulic transients applies to the liquid water remaining in the conduit, where the compression and rarefactions that travel back and forth in the liquid water (illustrated in Fig. 18b) are the precursor rarefactions due to surface unloading (illustrated in Fig. 7b). The resonant frequencies are about $f = a/4L$, and will increase with time as the water

column length, L, decreases. (Unfortunately, equipment used to date does not allow monitoring of frequencies above 60 Hz, and thus the progressive disappearance of the water column cannot be followed in detail. New equipment has been constructed to allow this experiment to be done.) Three important consequences of this explanation of the eruption wave train are that: (1) the hydraulic transients that occur during an eruption exist in an essentially static liquid column under the erupting two-phase mixture; (2) the transients are detected by the seismometers because coupling of the liquid water to the ground remains good through that part of the eruption where liquid water exists; and (3) the disappearance of the eruption wave train should coincide with the disappearance of liquid water in the conduit.

When an eruption starts, the flow is unsteady. In that part of the conduit where decompression has set a two-phase fluid into motion, Q changes from the recharge value of 5.7×10^3 cm^3 s^{-1} to about 1.13×10^5 cm^3 s^{-1}. The sound speed of the two-phase fluid is dramatically lower than that of liquid water, but its value cannot be accurately specified because of lack of field and laboratory data. A value of 50 m s^{-1}, appropriate to a nonequilibrium mixture at a few (less than 5) bars pressure and a few weight percent of vapor (Fig. 9a), is not unreasonable. When the entire fluid column has been converted to the two-phase mixture, the effective organ pipe for resonance extends from the ground surface to the top of the lower storage reservoir, 18 m. Therefore, the relative values of characteristic and hydraulic impedances are $Z_c = 5 \times 10^{-4}$ and $Z_h = 3.2 \times 10^{-2}$. The increase in flow rate due to eruption causes the hydraulic impedance to decrease. However, the hydraulic impedance is still greater than the characteristic impedance because the equally dramatic decrease in sound speed decreases the characteristic impedance. The characteristic frequencies of the flowing two-phase column are still the "closed pipe" frequencies, and are of order 1 Hz. Seismiticy at this frequency has not been detected during this stage of an Old Faithful eruption (Iyer and Hitchcock, 1974). However, strong pulsations of the water column at frequencies of 1—2 Hz are observed (Figs. 2 and 3) and these may reflect the resonant frequencies of the two-phase column.

The resonant frequencies of the two-phase column may be seismically undetectable because the transformation of the entire fluid column may result in acoustic decoupling of the fluid from the wall rocks (see Fig. 19b). The principles of this decoupling are the same as discussed above in the section on seismic quiet, i.e., acoustic disturbances in one substance cannot be detected by a detector in another substance unless there is a good impedance match with the substance in which the detector is placed.

In summary, the eruption wave trains of columnar geysers studied to date consist of harmonic tremor that appears to be due to hydraulic transients in liquid water remaining in their conduits underneath the discharging two-phase fluid. When the liquid water has been entirely converted to a water—steam mixture, the frequency of the tremor dramatically decreases. That the

difference in seismic behavior between columnar and fountain geysers coincides with the difference in eruption style suggests a basic difference in the triggering and eruption mechanisms for the two classes of geysers. Fountain geyser eruptions are basically triggered and sustained by bursts of individual bubbles of steam that move primarily through a liquid medium. In contrast, columnar geyser eruptions are triggered as a volume of water near the top of the column is brought onto the boiling curve, partially converted to steam, and ejected from the conduit, a process that allows water below to transform progressively into a two-phase state. Whereas the pressure disturbances in fountain geysers can be continuously transmitted to the wall rocks because liquid water is present as a transmitting medium, pressure disturbances in an erupting columnar geyser may cease to be transmitted to the wall rocks if the erupting fluid becomes entirely transformed into a two-phase fluid. These two types of geyser eruptions have analogies in Strombolian and Plinean eruptions respectively, and to the extent that the ideas in this paper can be extrapolated to volcanoes, analagous differences in seismic behavior should be expected.

SPECULATIONS ABOUT IMPLICATIONS OF THIS STUDY FOR VOLCANIC SEISMICITY

As mentioned in the Introduction, there are seismic events at volcanoes that are very similar to the pre-eruption seismic events ascribed to hydraulic transients at Old Faithful. Such events have a largely monochromatic frequency content, and varying durations and emergence characteristics. They have variously been called B-type volcanic earthquakes (Minikami, 1960, and many others), or low- or medium-frequency earthquakes (Latter, 1981). When they are sustained, or when many events produce a continuous train of waves, they merge into the phenomenon known as volcanic tremor, similar in apparent character to the eruption wave train at Old Faithful. The terms "B-type earthquakes" and "tremor" are by no means well-defined, and efforts to compare events of various common names at different volcanoes often fail. At the present time, the origins of B-type earthquakes, pre-eruption and eruption tremor are all controversial (e.g., Sassa, 1935, 1936; Kubotera, 1974; Steinberg and Steinberg, 1975; Aki et al., 1977; St. Lawrence and Quamar, 1979; Aki and Koyanagi, 1981; Chouet 1981; Seidl et al., 1981; Ferrick et al., 1982; Schick et al., 1982), but most of proposed mechanisms involve fluid motions within a volcanic edifice upon which the seismometers are located. Therefore, in spite of the possible differences in source mechanisms at different volcanoes, or at the same volcano at different times, a few speculations are suggested by this study:

Speculation 1: Liquid water can be a significant source of seismicity. One motivation for the present work was to study the cause of geothermal noise in a single, isolated system. The study suggests that hydraulic transients probably cause a large component of geothermal noise. In geothermal areas

the predominant frequencies are high (greater than 8 Hz in Yellowstone, Iyer and Hitchcock, 1974; about 2 Hz in the Imperial Valley, Douze and Sorrells, 1972; greater than 20 Hz at Solfatara Crater, Phlegraen Fields, Italy, Capello et al., 1974; and greater than 3 Hz in the Mt. Amiata geothermal area, Italy, DelPezzo et al., 1975). The high frequency characteristic of water-induced seismicity in these regions is probably due to the characteristically small dimensions of the near-surface fractures in these areas, where silica or other mineral deposition quickly seals fractures. The characteristic frequencies of 2—4 Hz at Karkar (Fig. 1a) are consistent with geothermal noise source dimensions on the order of L = 100 m.

There is no a priori reason to believe that water-induced tremor could not have lower frequencies than typical of shallow geothermal settings if conduits are appropriately long, as might be the case in tectonically active volcanic areas where new fractures would continually be created. On the other hand, it may be difficult to determine whether fluid-induced seismicity is due to magma or water, because the frequency is controlled by the sound speed of the fluid as well as the conduit dimensions. An interesting example where it may not be possible to determine from harmonic tremor alone whether the seismicity is water-induced or magma-induced is the 1–5 Hz tremor recently discovered in the underwater hydrothermal fields along the East Pacific Rise (Riedesel et al., 1982). The sound speeds of undersaturated liquid magma and pure liquid water are only a factor of two or three different; the sound speeds of the multiphase fluids that form when they saturate are comparably low. Therefore, various combinations of fluid sound speed and conduit length can give the observed tremor frequencies.

Speculation 2: The resonant frequencies of volcanic plumbing systems may change dramatically and shift outside the range of detectability of narrow-band seismometers. Many portable field seismometers have flat responses in a limited range between 1 and 40 Hz; this range was not sufficient to monitor tremor continuously as the pre-eruption bubble-quakes changed into eruption tremor at Old Faithful and Lone Star. Hence, this study suggests that seismographic systems for monitoring fluid-induced seismicity at volcanoes should be very broad band, capable of recording tremor frequencies that may span about two orders of magnitude as the magma acoustic velocity changes from kilometers per second in the liquid state to a few hundred meters per second in the vesiculated state.

Speculation 3: Apparent cessation of fluid-induced seismicity can occur for at least three reasons. (Note that cessation of tectonic seismicity, such as rock fracturing due to magma ascent, is *not* under consideration here.)

(a) The physical processes which drive the hydraulic transients recorded as seismic events may cease, as, for example, in the case of Old Faithful, when a rapid rise in water level temporarily suppresses steam bubble formation.

(b) The physical processes which drive the hydraulic transients may continue, but the resonant frequencies may have shifted out of the range of the detectors, as discussed above.

(c) The physical processes which drive the hydraulic transient may continue but the fluid may become acoustically decoupled from the rocks on which seismometers are placed because of state of the fluid has changed. The transformation of magma from an undersaturated liquid to a saturated liquid plus gas mixture would be the analogue of the transformation of liquid water to a liquid-plus-vapor mixture, and acoustic decoupling would be expected.

Speculation 4: The magnitude of eruption tremor may not, therefore, be a simple measure of the course of an eruption. A pre-requisite for seismic monitoring of hydraulic transients is a good, and constant, impedance match between the fluid in which the tremors are occurring and the host rock on which the seismometers rest. Such contact may exist in Hawaiian and Strombolian eruptions, where the eruptions consist of discrete or multiple gas bubbles rising through pools or conduits of liquid magma (like fountain geyser eruptions). However, at Plinian eruptions, there may be much more complex relation between eruption dynamics and seismicity. By analogy to Old Faithful it is likely during the course of a Plinian eruption the original immobile, essentially unvesiculated fluid becomes progressively more vesiculated and transforms to a fluid with dramatically different acoustic properties; this interpretation is supported by the theoretical models of Wilson (1980; and Wilson et al., 1980). Once this conversion has taken place, the fluid may not be capable of transmitting hydraulic transients to the wall rock because of the acoustic impedance mismatch.

Because of the hidden nature of the recharge and eruptive processes, these interpretations are highly speculative, even in the case of Old Faithful. However, the ideas presented are amenable to specific tests, and, at least at Old Faithful, future experiments may be able to reduce some of the speculation.

ACKNOWLEDGMENTS

This work was initially supported by the Kieffer personal bank account, then by a National Science Foundation Geochemistry grant to the author at UCLA, and then by the USGS Volcano Hazards and Geothermal programs. The field assistance of Sue Beard, Rick Hutchinson, Steve Ihnen, and Gonzolo Mendoza in obtaining the seismic data in Yellowstone, and Hugh and Bobby Kieffer in Iceland, is much appreciated. Much of the seismic equipment used in this study was built by Jerry Eaton, Ed Criley, and John Van Schaack, and discussions with M. Iyer and D. Stauber of the USGS aided in design of the seismic experiments and preliminary analysis of the data. The cooperation of the U.S. National Park Service is much appreciated. The author thanks the dozen colleagues who, over the four years of evolution of the manuscript, greatly clarified it by their unanimous skepticism.

REFERENCES

Aki, K. and Koyanagi, R., 1981. Deep volcanic tremor and magma ascent mechanism under Kilauea, Hawaii. J. Geophys. Res., 86: 7095–7109.

Aki, K., Fehler, M. and Das, S., 1977. Source mechanism of volcanic tremor: Fluid-driver crack models and their application to the 1963 Kilauea eruption. J. Volcanol. Geotherm. Res., 2: 259—287.

Bennett, F.D., 1971. Vaporization waves in explosive volcanism. Nature, 234: 538.

Bennett, F.D., 1972. Shallow submarine volcanism. J. Geophys. Res., 77: 5755.

Bennett, F.D., 1974a. On volcanic ash formation. Am. J. Sic., 274: 648.

Bennett, F.D., 1974b. Criteria for volcanic ash formation. In: Proc. of the Symp. on Andean and Antarctic Volcanology Problems. Chile, p. 48.

Birch, F., 1966. Compressibility, elastic constants. In: S.P. Clark (Editor), Handbook of Physical Constants. Geol. Soc. Am., Mem., 97: 97—173.

Birch, F. and Kennedy, G.C., 1972. Notes on geyser temperatures in Iceland and Yellowstone National Park. Geophys. Monog., Am. Geophys. Union, 16: 329—336.

Cappello, P., Lo Bascio, A. and Luongo, G., 1974. Seismic noise survey at Solfatara Crater, Phlegraean Fields, Italy. Geothermics, 3: 76—80.

Chouet, B., 1981. Ground motion in the near field of a fluid-driven crack, and its interpretation in the study of shallow volcanic tremor. J. Geophys. Res., 86: 5985—6016.

Del Pezzo, E., Guerra, I., Luongo, G. and Scarpa, R., 1975. Seismic noise measurements in the Mt. Amiata geothermal area, Italy. Geothermics, 4: 40—43.

Douze, E.J. and Sorrells, G.G., 1972. Geothermal ground-noise surveys. Geophysics, 37: 813—824.

Ferrick, M.G., Quamar, A. and St. Lawrence, W.F., 1982. Source mechanism of volcanic tremor. J. Geophys. Res., 87: 8675—8683.

Fournier, R., White, D. and Truesdell, A., 1976. Convective heat flow at Yellowstone National Park, Wyoming. Proc. of the Second United Nations Symposium on the Develop. and Use of Geothermal Resources, pp. 731—740.

Fujikawa, S. and Akamatsu, T., 1978. Experimental investigations of cavitation bubble collapse by a water shock tube. Bull. Jpn. Soc. Min. Eng., 21: 223—230 and 279—281.

Iyer, H.M. and Hitchcock, T., 1974. Seismic noise measurements in Yellowstone National Park. Geophysics, 39: 389—400.

Kieffer, S.W., 1975. Geysers: A hydrodynamic model for the early stages of eruption. Geol. Soc. Am. Abstr. Progr., 7 (7): 1146.

Kieffer, S.W., 1977a. Fluid dynamics during eruption of water—steam and magma—gas systems: geysers, maars and diatremes. Second International Kimberlite Conference, Santa Fe, New Mexico, Abstracts, no pages listed.

Kieffer, S.W., 1977b. Sound speed in liquid—gas mixtures: water—air and water—steam. J. Geophys. Res., 82: 2895—2904.

Kieffer, S.W., 1982. Geyser eruptions: Characteristics and mechanisms, with emphasis on Old Faithful Geyser, Yellowstone National Park, and Mount St. Helens, March—April, 1980. 1982 IAVCEI Symposium on Generation of Major Basalt Types, Aug. 15—22, 1982, Reykjavik, Iceland, No. 102.

Kieffer, S.W. and Delany, J.M., 1979. Isentropic decompression of fluids from crustal and mantle pressures. J. Geophys. Res., 84: 1611—1620.

Kieffer, S.W. and Ihnen, S., 1977. Seismic and aseismic geyser eruptions. EOS Trans. Am. Geophys. Union, 58 (12): 1187.

Kubotera, A., 1974. Volcanic tremors at Aso Volcano. Dev. Solid Earth Geophys., 6: 29—47.

Latter, J.H., 1981. Volcanic earthquakes, and their relationship to eruptions at Ruapehu and Ngauruhoe volcanoes. J. Volcanol., Geotherm. Res., 9: 293—310.

McKee, C.O., Wallace, D.A., Almond, R.A. and Talais, B., 1981. Fatal hydro-eruption of Karkar volcano in 1979: development of a maar-like crater. In: R.W. Johnson (Editor), Cookre-Ravian Volume of Volcanological Papers. Geol. Surv. Papua New Guinea, Mem., 10: 63—84.

Minakami, T., 1960. Fundamental research for predicting volcanic eruptions (I) — earthquakes and crustal deformations originating from volcanic activities. Bull. Earthquakes Res. Inst., Univ. Tokyo, 38: 497—547.

Nicholls, H.R. and Rinehart, J.S., 1967. Geophysical study of geyser action in Yellowstone National Park. J. Geophys. Res., 72: 4651—4663.
Riedesel, M., Orcutt, J.A., MacDonald, K.C. and McClain, J.S., 1982. Microearthquakes in the Black Smoker Hydrothermal Field, East Pacific Rise at 21°N. J. Geophys. Res., 87: 10613—10623.
Rinehart, J., 1969. Old Faithful Geyser. Physics Teacher, 7: 221—224.
Rinehart, J.S., 1974. Geysers. EOS, Trans. Am. Geophys. Union, 55: 1052.
Rinehart, J.S., 1980. Geysers and Geothermal Energy. Springer-Verlag, New York, N.Y., 223 pp.
Sassa, K., 1935. Volcanic micro-tremors and eruption-earthquakes. Mem. Coll. Sci., Kyoto Univ., 18 (5): 255—294.
Sassa, K., 1936. Micro-seismometric study on eruptions of the volcano Aso. Mem. Coll. Sci., Kyoto Univ., 19 (1): 11—56.
Schick, R., Lombardo, G. and Patane, G., 1982. Volcanic tremors and shocks associated with eruptions at Etna (Sicily), September 1980. J. Volcanol. Geotherm. Res., 14: 261—279.
Seidl, D., Schick, R., and Riuscetti, M., 1981. Volcanic tremors at Etna: a model for hydraulic origin. Bull. Volcanol., 44: 43—56.
Stanyukovich, K.P., 1960. Unsteady Motion of Continuous Media, English transl. by M. Holt, ed., Pergamon Press, New York, N.Y., 745 pp.
Steinberg, G.S. and Steinberg, A.S., 1975. On possible causes of volcanic tremor. J. Geophys. Res., 80: 1600—1604.
St. Lawrence, W. and Quamar, A., 1979. Hydraulic transients: a seismic source in volcanoes and glaciers. Science, 203: 654.
Thompson, P.A., 1972. Compressible-fluid Dynamics. McGraw-Hill, New York, N.Y., 665 pp.
White, D.E., 1967. Some principles of geyser activity mainly from Steamboat Springs, Nevada. Am. J. Sci., 265: 641—684.
White, D.E., Fournier, R.O., Muffler, L.J.P. and Truesdell, A.H., 1975. Physical results of research drilling in thermal areas of Yellowstone National Park, Wyoming. U.S. Geol. Surv., Prof. Pap., 892, 70 pp.
Wilson, L., 1980. Relationships between pressure, volatile content and ejecta velocity in three types of volcanic explosion. J. Volcanol. Geothermal Res., 8: 297—313.
Wilson, L., Sparks, R.S.J. and Walker, G.P.L., 1980. Explosive volcanic eruptions. IV. The control of magma properties and conduit geometry on eruption column behavior. Geophys. J. R. Astron. Soc., 63: 117—148.
Wylie, E.B. and Streeter, V.L., 1978. Fluid Transients, McGraw-Hill, New York, N.Y., 384 pp.